The rate of environmental fluctuations shapes ecological dynamics in a two-species microbial system

Alejandra Rodríguez-Verdugo[1,2,3,*], Clément Vulin[1,2] and Martin Ackermann[1,2]

[1] Department of Environmental Systems Sciences, ETH Zürich, Zürich, Switzerland

[2] Department of Environmental Microbiology, Eawag, Dübendorf, Switzerland

[3] Adaptation to a Changing Environment, ETH Zürich, Zürich, Switzerland

Clément Vulin

E-MAIL: clement.vulin@eawag.ch

Martin Ackermann

E-MAIL: martin.ackermann@env.ethz.ch

[*] Corresponding author:

Alejandra Rodríguez-Verdugo

E-MAIL: alejandra.rodriguez@eawag.ch

MAILING ADDRESS:

Eawag, Dept. of Environmental Microbiology

Überlandstrasse 133

8600 Dübendorf

Switzerland

TELEPHONE: +41 58 765 5996

FAX: +41 58 765 5802

This document is the accepted manuscript version of the following article:

Rodríguez-Verdugo, A., Vulin, C., & Ackermann, M. (2019). The rate of environmental fluctuations shapes ecological dynamics in a two-species microbial system. Ecology Letters, 22(5), 838-846. https://doi.org/10.1111/ele.13241

Statement of authorship: All the authors conceived and designed the study. ARV conducted the experiments and collected the data. CV built the mathematical model. ARV and CV analyzed the data. ARV wrote the initial draft of the manuscript while MA and CV provided substantial feedback. All authors gave final approval for publication.

Data accessibility statement: Upon manuscript acceptance, all data and codes generated in this study will be available in Dryad and the data DOI will be included at the end of the article.

Running title: Community dynamics in changing environments

Keywords: Synthetic communities, species interactions, population dynamics, rate of environmental change, mathematical modeling, cross-feeding, *Acinetobacter johnsonii*, *Pseudomonas putida*, resource competition, exploitation

Type of article: Letters

Number of words in the abstract: 144

Number of words in the main text: 4994

Number of references: 32

Number of figures and tables: 3 figures and 2 tables

Abstract

Species interactions change when the external conditions change. How these changes affect microbial community properties is an open question. We address this question using a two-species consortium in which species interactions change from exploitation to competition depending on the carbon source provided. We built a mathematical model and calibrated it using single-species growth measurements. This model predicted that low frequencies of change between carbon sources lead to species loss, while intermediate and high frequencies of change maintained both species. We experimentally confirmed these predictions by growing co-cultures in fluctuating environments. These findings complement more established concepts of a diversity peak at intermediate disturbance frequencies. They also provide a mechanistic understanding for how the dynamics at the community level emerges from single-species behaviors and interspecific interactions. Our findings suggest that changes in species interactions can profoundly impact the ecological dynamics and properties of microbial systems.

Introduction

Microbial communities live in ever-changing environments. First, microbes are constantly exposed to fluctuations in physical and chemical factors such as temperature, pH, UV radiation and moisture. Second, they experience changes in the resources they need to grow and divide. For example, it is common that bacteria experience periods of resource abundance followed by periods of scarcity (i.e. 'feast and famine' fluctuations; Vasi et al. 1994). Bacteria not only experience fluctuations in the amount but also in the type of resources. For example, leaf microbial populations feed on methanol produced by the plant during the morning and then switch to other carbon sources later in the day (Vorholt 2012). Given that changes in resources are common in nature and that they affect the reproduction and survival of microorganisms, it is important to understand how these changes affect microbial communities. More broadly, it is fundamental to understand how the rate of environmental change affects community properties (e.g. species diversity, richness abundance, stability) and to what extent temporal changes in the environment shape population dynamics in microbial communities.

Understanding the role of environmental fluctuations on community properties has been of central interest to ecologists for decades (Connell 1978; Chesson 2000; Barabás et al. 2018). One aspect that has received a lot of attention is how different frequencies of environmental fluctuations affect community properties (Miller et al. 2011; Yi & Dean 2013). A prevalent idea in the literature is that there is an intermediate frequency of change that maximizes species diversity and abundance. For example, the 'Intermediate Disturbance Hypothesis' states that species diversity should be higher at intermediate frequencies and/or intensities of disturbance (Connell 1978). The intermediate disturbance hypothesis has been criticized, in part because it lacks empirical support (Mackey & Currie 2001) and, in

87 part, because it lacks a mechanistic description of the processes that underlie community
88 dynamics (Fox 2013). Furthermore, this hypothesis assumes that: 1) the interaction
89 between species does not change in time and 2) competition is the predominant type of
90 interactions. However, species interactions in natural communities are constantly changing
91 in response to environmental fluctuations, such as changes in the type and amount of
92 resources (Dolinšek et al. 2016). Therefore, changes in species interactions should be
93 incorporated in this type of ecological models.
94 In this study we revisited the general idea that different frequencies of
95 environmental change affect community properties while aiming to attain a mechanistic
96 understanding of species interactions. In particular, we studied a simple system in which
97 interactions between two species change in function of the environmental conditions, i.e.
98 the type of resource provided. In one condition, species stably coexisted through cross-
99 feeding of resources while, in the other condition, species competed for a limiting resource.
100 We simulated a simple scenario in which the environment alternates between these two
101 conditions at different frequencies and hypothesized that different frequencies of change
102 impact species abundance and coexistence. First, we hypothesize that low frequencies of
103 change would result in species loss given that species are prone to competitive exclusion in
104 the competition condition. Second, high frequencies of change could also lead to species
105 loss given that each time the conditions change, organisms have to induce different sets of
106 genes to metabolize the available resource and this metabolic switching might not be fast
107 enough to keep up with the fluctuations in the resource (Turkarslan et al. 2017). Finally,
108 intermediate frequencies of change could allow species coexistence.
109 To test these hypotheses, we used a bottom-up approach based on a synthetic
110 community of low complexity. Synthetic communities offer advantages that are relevant

here: 1) they offer a high degree of experimental control and replication and, 2) they allow gaining a mechanistic understanding of interspecies interactions (De Roy et al. 2014). The synthetic community used in this study was composed by two species: *Acinetobacter johnsonii* C6 and *Pseudomonas putida* KT2440 (Hansen et al. 2007b; Haagensen et al. 2015). We chose these two species because they are able to assimilate a wide range of substrates, including aromatic compounds that can potentially pollute the environment. One of these aromatic compounds is benzyl alcohol, which can be used as sole source of carbon and energy by *A. johnsonii* but not by *P. putida*. Instead, *P. putida* can use benzoate, which is a by-product excreted by *A. johnsonii* during the oxidation of benzyl alcohol. Therefore, in a medium supplemented with benzyl alcohol, *A. johnsonii* and *P. putida* coexist by feeding on benzyl alcohol and benzoate, respectively. For the competition condition, we supplemented the medium with citrate which is a non-aromatic compound that both species can use as source of carbon and energy. We coupled this experimental approach with mathematical modeling, first to test if we could infer community dynamics from single-species behaviors and second to test how different frequencies of environmental change affect community properties.

Materials and Methods

Strains

A. johnsonii strain C6 was originally isolated from a creosote-polluted aquifer and is naturally resistant to streptomycin (Kaas et al. 2017). We used a strain of *P. putida* KT2440 unable to metabolize benzyl alcohol (absence of the TOL or pWW0 plasmid) and resistant to gentamycin (based on a gfp-Gm^r cassette inserted onto its chromosome; Hansen et al.

2007a). The strains were kindly provided by Søren Molin and Sünje Johanna Pamp from the Technical University of Denmark, Kongens Lyngby, Denmark.

Growth conditions

Strains were grown in AB minimal medium (1 mM $MgCl_2$, 0.1 mM $CaCl_2$, 0.003 mM $FeCl_3$, 15 mM $(NH_4)_2SO_4$, 33mM Na_2HPO_4, 22 mM KH_2PO_4, and 50 mM NaCl) supplemented with one of the following carbon sources: 0.6 mM benzyl alcohol, 1 mM sodium benzoate or 1 mM citrate. All solutions were filter-sterilized using filters that were washed with one liter of deionized water to remove traces of carbon in the filters.

Batch culture experiments

We grew our bacteria in batch culture in which the resources are initially abundant but eventually get depleted. After 24 hours of bacterial growth, 1% of the population was diluted into a batch of fresh medium (i.e. 100-fold dilution). For a culture to sustain the 100-fold dilution regime, the population must achieve approximately 6.64 generations of binary fission per day ($\log_2(100)$). We repeated these passages for 6 days and we did this experiments in monoculture (growing species in isolation) or in co-cultures (growing the species in pairs).

Batch cultures were grown in 40 ml glass vials with screw caps containing TFE-lined silicone septa. Vials and screw caps were treated to eliminate any trace of contaminant carbon that could sustain bacterial growth; i.e. assimilable organic carbon (AOC). AOC-free material was prepared as in (Hammes & Egli 2005): vials were submerged overnight in 0.2 N HCl and rinsed twice with deionized water. To remove all trace organics, vials were heated in a Muffle oven to 500°C for 3 h. Screw caps were soaked in a 10% sodium persulfate solution at 60°C for 1 h, rinsed twice with deionized water and air-dried.

We started each experiment by isolating a single colony and growing it in 3 ml of LB broth supplemented with antibiotics. We incubated the cultures overnight at 30°C with constant shaking (220 rpm). The next day, we washed the cells to remove any excess of LB and antibiotics by spinning down 1 ml overnight culture and washing three times with AB medium without carbon source. Washed cells were diluted 10,000-fold into 10ml fresh AB medium supplemented with the desired carbon source and incubated for one day at 30°C and shaken at 150 rpm. These cultures were then diluted 100-fold into 10 ml fresh AB medium supplemented with the desired carbon source to start the monocultures, or were mixed at a 1:1 volumetric ratio and diluted 100-fold into 10 ml media to start the co-cultures. Initial population sizes were approximately 10^5 cells per species. Monocultures and co-cultures were propagated by daily transfers of 0.1 ml of culture into 9.9 ml of fresh medium for 6 days. At the end of each day, population densities of *A. johnsonii* and *P. putida* were estimated by plating on Luria-Bertani (LB) agar supplemented with streptomycin (64 µg/ml) and gentamicin (10 µg/ml), respectively.

Estimation of ecological interactions from batch culture experiments

We characterized the ecological interaction between species by analyzing the dynamics from our batch culture experiments. We aimed to differentiate among three types of interactions: 1) a **commensal interaction** in which one species benefits from the interaction, whereas the other species neither benefits nor suffers from the interaction (+,0), 2) a **exploitative interaction** in which one species benefits from the interaction while harming the other species (+,-), and 3) a **competitive interaction** in which both species suffer from the interaction (-,-). To define the type of interaction between species we first

estimated the slope of the linear regression between time (over 6 days) and the $\log_{10}$ of the densities estimated at the end of the 24 hours growth cycle, based on three replicates. If the slopes were not significantly different from 0, we concluded the populations were able to overcome a 100-fold dilution regime and were stable over the course of the experiment. We then compared the population densities over 6 days for each species in monocultures and co-cultures and performed a t-test over the means. If the densities were not significantly different in monocultures and in co-cultures we concluded that species had a neutral interaction. All the statistical analyses were done using R (version 3.2.3).

Mathematical model to predict community behaviors

We built a mathematical model that explicitly modelled the changes in resources and the bacterial growth. We used single-species growth measurements to parameterize the model. We estimated five parameters that we considered relevant to predict the dynamics in batch culture: 1) the **maximum growth rate** in exponential phase, 2) the **maximum uptake rate** corresponding to the saturated uptake rate for high resource concentration, 3) the **half-saturation constant** defined as the resource concentration supporting half-maximum uptake rate, 4) the **duration of the lag phase** defined as the time bacteria spend in a non-growing state after being transferred into fresh medium and before they resume growth and 5) the **excretion rate proportionality factor** as a proxy of how much benzoate is excreted to the medium.

We estimated all the parameters except for the benzoate excretion rate using optical density (OD) measurements from plate reader experiments. Bacteria were acclimated to their assay condition as previously described for the beginning of the serial

dilution experiment. We transferred 2µl of the saturated culture intro 198µl of fresh media dispensed in each of the wells of the 96-wells plate. To avoid evaporation, we covered the plates with a lid, which we sealed with silicon grease. We incubated the plates at 30°C with constant shaking inside a photospectrometer (Eon™, BioTek™), which lowest detection limit was 0.003. OD measurements were acquired every 5 minutes for 24 hours. We replicated the experiments three times. Each parameter was fitted to three growth curves (i.e. three technical replicates) and the average was used to parameterize the model. All the fitting of parameters was done using Matlab (version R2017a, Mathworks).

Maximum growth rates – To estimate the maximum growth rate, μ_{max}, we fitted a linear regression to the natural logarithm of the OD over time during the exponential growth phase.

Maximum uptake rates and half-saturation constants – To estimate the maximum uptake rate (*V*) and the half-saturation constant (*K*) we used the growth curves data (Fig. S1). We first estimated the yield (i.e., the amount of biomass produced per unit of resource) using the following relationship (1):

$$Y = \frac{OD_{max} - OD_{min}}{R_0}$$

where OD_{max} is the maximum OD after saturation, OD_{min} is the minimum OD at the start of the experiment and R_0 is the initial concentration of resource used in each condition (i.e. 0.6 mM of benzyl alcohol and 1 mM of citrate). The final concentration of resource was assumed to be negligible. We then modeled the uptake rate (i.e. the rate of resource consumption per hour) using the following relationship (2):

$$q = \frac{\mu}{Y}$$

where μ is the instantaneous growth rate (h^{-1}), calculated as Δ ln(OD)/ Δ t, and Y is the yield calculated with the relationship (1). We assumed the yield was constant over the entire growth period (Monod 1942).

We then modeled the change in resources over time using the following relationship (3):

$$\frac{dR}{dt} = -\frac{1}{Y}\frac{dX}{dt}$$

where *X* is the bacterial density (OD) and Y is the yield. Finally, we plotted the uptake rate in function of the changes in the resources and fitted the maximum rate of the uptake reaction (*V*) and the half-saturation constant (*K*) using the following relationship (4):

$$q(R) = \frac{V\,R}{K + R}$$

Duration of lag phase - We defined the duration of the lag phase by regression of an exponential growth model on the OD measurement to the calculated initial OD value. We acclimated a culture to a given carbon source as previously described and then transferred 2 µl of the saturated culture into 198 µl of fresh media containing a different carbon source. During the same experiment, we filled some wells with the acclimated cultures used for the experiment and measured their OD. This final OD was used to infer the initial theoretical OD at the beginning of the growth experiment (the real initial OD measurements were below the detection level of the instrument and could not be directly measured).

Benzoate excretion rate – We estimated the benzoate excretion rate from metabolite measurements. We quantified how much benzoate was excreted to the medium by *A. johnsonii* using high performance liquid chromatography (HPLC). We grew a 20 ml monoculture of *A. johnsonii* in 0.6 mM benzyl alcohol for 24 hours. We sampled the growing culture approximately every hour by taking 1 ml of culture and filtering it through a 0.2 µm-pore-size filter. Samples were immediately analyzed with a Summit HPLC system (Dionex)

248 with a Triart C18 revered phase column (250 x 4.6 mm) and with a UVD340U photodiode
249 array detector. The mobile phase was a solution of 60% PO_4 (50 mM, pH 3.0 HCl) and 40%
250 acetonitrile, supplied at a flow rate of 1 ml/min. We replicated the experiments three times.
251 To estimate the rate of consumption of benzyl alcohol and the rate of production of
252 benzoate we fitted a linear regression to the natural logarithm of the metabolites
253 concentration over time during exponential consumption/production. Finally, the excretion
254 rate was inferred from the fact that the amount of benzoate produced and excreted to the
255 medium is proportional to how much *A. johnsonii* grows on benzyl alcohol (differential
256 equations in Table 1). The value of this proportionality factor, α, was therefore quantified by
257 dividing the rate of production of benzoate by the rate of consumption of benzyl alcohol.

258 **Explicit modeling of the resource**

259 We used Matlab's ODE45 solver (version R2017a, Mathworks), which is a single step
260 solver based on an explicit Runge-Kutta formula (Dormand & Prince 1980; Shampine &
261 Reichelt 1997). Bacteria and resources concentrations were modeled with differential
262 equations (Table 1). Each time bacteria changed media, a fixed population lag time was
263 implemented, and at each dilution, $1/100^{th}$ of the media containing the bacteria was
264 transferred into fresh media. Our model assumed no mortality over a 24-hour cycle, which
265 was supported by experimental observation (data not shown). Finally, we added an
266 extinction factor in which extinction was occurring when the probability of transferring
267 fewer than one bacterium in the sampling Poisson process was over 50%.

268 Finally, to be able to compare the results generated by our model to our
269 experimental data, we converted the numerical values generated by the model (in OD units)
270 to estimates of cell numbers (measured as 'colony forming units', CFU). To do so, we used a
271 saturated culture of *A. johnsonii* and *P. putida* and diluted it so we had two, four and eight-

fold dilutions. We measured the OD of the undiluted and diluted cultures in the plate reader and plated them in LB agar to estimate their CFU. We replicated the experiment three times. We used the slope of the linear relationship between the OD and the cell density as the conversion rate (Fig. S2).

Results

Interactions between species change depending on the carbon source provided

To study the dynamics of microbial interactions in fluctuating environments we established an experimental system in which we could modulate species interactions. We used a previously characterized two-species consortium composed of *A. johnsonii* C6 and *P. putida* KT2440 (Hansen et al. 2007b). These two species engage in a cross-feeding interaction when grown in benzyl alcohol as sole carbon source. *A. johnsonii* feeds on benzyl alcohol and metabolizes it into benzoate. Some of the benzoate accumulates inside the cells and then leaks into the environment where *P. putida* consumes it. This cross-feeding interaction had been reported in chemostats and biofilms but has not been analyzed in batch cultures in which the concentration of nutrients varies seasonally (i.e. 'feast and famine' regime).

First we tested if we could establish this metabolic interaction in a batch culture system. To do so, we grew monocultures and co-cultures of *A. johnsonii* and *P. putida* in minimal medium supplemented with 0.6 mM benzyl alcohol, starting from an initial population density of 10^5 colony-forming units per ml (CFU/ml) for each species. After 24 hours, we transferred 1% of the populations to fresh medium and repeated this daily growth cycle for six consecutive days, using three independent replicate populations. Each

294 day, we plated samples of the liquid cultures and counted the resulting colonies, so that we
295 could analyze population sizes of both species over time.
296
297 We first analyzed population sizes in monocultures grown on 0.6 mM benzyl alcohol
298 (Fig. 1A). *A. johnsonii* reached a high and stable density of approximately $3.1*10^7$ CFU/ml ±
299 $3.7*10^6$ CFU/ml (mean ± standard error of the mean; slope of the linear regression of the log
300 final CFU over six days = -0.02 day^{-1}; 95% upper CI = 0.06 day^{-1}). In contrast, *P. putida*
301 densities dropped after the first two transfers but stabilized, reaching a low population
302 density of approximately $3.6*10^4$ CFU/ml ± $1.5*10^4$ CFU/ml (Fig. 1A; slope of linear
303 regression = -0.14 day^{-1}; 95% upper CI = 0.01 day^{-1}). Additional experiments suggested that
304 *P. putida* could maintain this density by growing on residues of organic carbon that were
305 inadvertently present in the culture medium (Fig. S3).
306
307 Then, we analyzed population sizes in co-cultures of *A. johnsonii* and *P. putida* grown on 0.6
308 mM benzyl alcohol. *P. putida* achieved approximately $1.8*10^6$ CFU/ml ± $1.5*10^4$ CFU/ml,
309 that is, a density that is fifty times higher than in monocultures (two-tailed *t*, df = 17, and *P* <
310 0.001, Fig. 1A), despite a slight but significant decrease in population densities (slope of
311 linear regression = -0.12 day^{-1}; 95% upper CI = -0.002 day^{-1}). Therefore, the presence of *A.*
312 *johnsonii* promoted the growth of *P. putida* presumably based on benzoate cross-feeding. *A.*
313 *johnsonii* sustained slightly but significantly lower densities in co-cultures ($3.1*10^7$ CFU/ml ±
314 $3.7*10^6$ CFU/ml in monocultures; $1.7*10^7$ CFU/ml ± $2.3*10^6$ CFU/ml in co-cultures; two-
315 tailed *t*, df = 28, and *P* = 0.004), suggesting *P. putida* had a negative effect on *A. johnsonii* in
316 benzyl alcohol. Therefore, we concluded *P. putida* and *A. johnsonii* had an exploitative
317 interaction (+,-) in benzyl alcohol.

Next, we set up a condition in which both species would compete for a limiting resource. We used citrate as limiting carbon source. When grown in 1 mM citrate, both species in monocultures could sustain high densities of approximately $5*10^7$ CFU/ml (Fig. 1B). In contrast, in co-cultures only *P. putida* reached high cell densities while *A. johnsonii* was diluted to extinction after the fourth transfer (slope of the linear regression = -1.6 day^{-1}; 95% upper CI = -1.3 day^{-1}). *P. putida* sustained similar population densities in monocultures and in co-cultures ($5.3*10^7$ CFU/ml ± $1.1*10^7$ CFU/ml in monocultures; $7.6*10^7$ CFU/ml ± $2*10^7$ CFU/ml in co-cultures; two-tailed *t*, df = 27, and *P* = 0.337). Therefore, *A. johnsonii* and *P. putida* had a highly asymmetric competitive interaction (-,-). These results establish that we were able to tune ecological interactions by providing different carbon sources. Specifically, we imposed exploitation in benzyl alcohol and competition in citrate.

Mathematical model predicts different community dynamics when the environment changes at different frequencies

After engineering a system in which ecological interactions change from exploitation to competition as a function of the carbon source provided, we asked how changing these carbon sources at different frequencies would affect community dynamics. To address this question, we built a mathematical model using data collected from monocultures to derive specific predictions that could be tested with experiments in co-cultures. Our ultimate goal was to test if we could accurately predict community dynamics from a mechanistic understanding on single-species behavior. To build a mathematical model, we estimated five parameters - the maximum growth rate μ_{max}, the maximum resource uptake rate *V*, the half-saturation constant *K*, the duration of the lag phase λ and the benzoate excretion rate -

341 from monoculture growth curves and metabolite analysis (Table 2, Fig. S4 and Fig. S5). The
342 growth of each species was dependent on the concentration of resources, which we
343 modeled explicitly (Table 1). We incorporated the duration of the lag time of *A. johnsonii*
344 when changing between carbon sources (Table 2). In addition, we incorporated the daily
345 dilution that resulted from transferring 1/100 of the culture into fresh media. The bacteria
346 were considered extinct when they reached an extinction threshold (Material and
347 Methods).
348
349 Our model was able to capture the ecological dynamics of co-cultures of the two
350 species in constant environments that we observed previously (Fig. S6). This suggested that
351 the ecological dynamics in our system are mostly driven by resource utilization (i.e. cross-
352 feeding of resources or competition for resources). Having confirmed that we had a
353 mechanistic understanding of our system, our next goal was to use the model to predict the
354 ecological dynamics in conditions where the external environment fluctuates. We simulated
355 different frequencies of changes between carbon sources, from daily fluctuations to five
356 days fluctuations, always starting with citrate as carbon source. These simulations predicted
357 that rapid (1-2 days) and intermediate (3 days) fluctuations allow species coexistence (Fig.
358 2). In contrast, slow changes (4-5 days fluctuations) are predicted to lead to the extinction of
359 one of the two species, *A. johnsonii*, after three transfers. When we ran the model for 8 and
360 10 days (equivalent to two full cycles of citrate and benzyl alcohol), *P. putida* was diluted to
361 extinction after 6 and 7 transfers in the 4 and 5-days fluctuating regime, respectively.
362 Overall, the model predicted that the rate of environmental change modulated species
363 richness and abundance. If the environment fluctuated with a slow frequency of change, the

relative amplitude between species abundances got large until the first species went extinct, followed by the extinction of its exploitative partner.

Experimental data confirm the community dynamics generated by the mathematical model

The mathematical model allowed us to predict community dynamics in fluctuating environments using data collected from monocultures. We tested the validity of these predictions by doing experiments in co-cultures, in fluctuating environments. We started co-cultures with a ratio of 1:1 of each species, at a population density of 10^5 CFU/ml. We did our serial dilution experiment for six consecutive days, using three independent replicate populations. We tested the same fluctuating conditions as we simulated with the model. As predicted by the model, we found that fast and intermediate fluctuations allow species coexistence, with larger amplitude of relative abundances change in intermediate fluctuating environments (Fig. 3). In the 4-days fluctuating environment, *A. johnsonii* was diluted to extinction after three transfers for two of the replicates. In one replicate, we observed a sudden recovery of *A. johnsonii* after four transfers when the environment changed back to benzyl alcohol (Fig. 3). In the 5-days fluctuating regime, in all three replicates, *A. johnsonii* went extinct over the course of the experiment. We continued the experiment over 10 days for one of the replicates but did not observed the extinction of *P. putida*, which was predicted by the model. With the exception of the unexpected long-term persistence of *P. putida*, we were able to accurately predict ecological community's dynamics from parameters measured in monocultures.

Discussion

We have established a system in which we can modulate interspecies interactions by changing the carbon source provided. Using a mathematical model, we have accurately predicted community dynamics from single-species growth measurements, establishing that it is possible to predict community-level properties based on population-level properties. Finally, we have shown that different frequencies of environmental change affect community composition and stability.

Interspecies interactions are highly dynamic

Interspecies interactions change depending on the carbon source provided. In a minimal medium supplemented with benzyl alcohol as sole carbon source, *P. putida* exploits *A. johnsonii* (+,-). In contrast to our study, their interaction have been previously described as commensal (+,0); that is *P. putida* benefits from the presence of *A. johnsonii* and *A. johnsonii* is not affected by the presence of *P. putida* (Hansen et al. 2007b). This discrepancy between studies may be explained by the supply of resources. When the resources are supplied continuously a commensal interaction is sustained though cross-feeding. When the resources are supplied in pulses the interaction changes from commensal to exploitative when the nutrients are exhausted from the medium (Fig. S5). In conclusion, by growing a previously characterized consortium in an environment with seasonal changes of nutrient concentrations, we have observed a different type of interactions. Shifts in species interactions due to nutrient availability changes have been previously observed for different genotypes of the same microbial species (Hoek et al. 2016), but have been less investigated for different species (Jagmann et al. 2010). This suggests a need for more studies that

carefully characterize – and quantify – interspecies interactions in different nutrient regimes.

In conclusion, we have shown that species interactions are highly dependent on the environmental context. Given that natural environments are constantly changing, presumably species interactions in nature are also expected to constantly change. Acknowledging how dynamic are species interactions can provide valuable insights into fundamental questions in community ecology, such as: can we model complex microbial communities to predict their behavior in real-world situations? Microbial community models usually assume that species interactions are static; e.g. interaction networks are often snapshots of the state of a community at a particular time and place (Faust & Raes 2012). Implementing dynamic models of microbial interactions will provide better insights into our understanding on how communities function and respond to environmental changes.

Community-level properties can be predicted from population-level properties

An important challenge in ecology is to infer community-level properties from population-level properties, i.e. predicting community dynamics from single-species behaviors (Megee et al. 1972; Lee et al. 1976; Hansen & Hubbell 1980). In this study we have added to previous literature by showing this is possible. We have accurately predicted short-term community dynamics using a mathematical model and fitting parameters from monocultures. This was likely possible because interactions between species were based on resource interactions. Recent studies combining mathematical modeling with experiments but using different microbial systems, have also being able to capture community dynamics from single-species behaviors (Louca & Doebeli 2015; Hanemaaijer et al. 2017; Hart et al.

2018). A common conclusion among studies is that accurate predictions were only possible based on a good mechanistic understanding of the system. Therefore, we are optimistic we will be able to predict community dynamics for complex microbial systems if we understand how species interact in these systems, which can be achieved by combining top-down and bottom-up approaches with mathematical modeling.

It is worth nothing that we did not accurately predict the long-term community dynamics. The model predicted the extinction of *P. putida* after 8 transfers in a six-days fluctuating regime, but we observed the persistence of *P. putida* at low densities (Fig. S7). We have two hypotheses to explain this observation. Our first hypothesis is that *P. putida* can maintain a low density by growing on residues of organic carbon that were inadvertently present in the culture medium. Our second, nonexclusive hypothesis is that *P. putida* rapidly evolved to utilize these residues. Although we do not yet know the precise mechanism underlying the persistence of *P. putida*, both hypotheses can be implemented in a mathematical model. More generally, the discrepancies between the model and the experimental data highlight the importance of incorporating evolutionary dynamics into ecological models.

The rate of environmental change is relevant for stability and maintenance of a two-species consortium

In this study we have revisited the idea that, in fluctuating environments, there is an intermediate frequency of environmental change that maximizes species diversity and stability. We have shown that low frequencies of environmental change lead to species loss, while intermediate and fast frequencies of environmental change maintain coexistence of

two species. Although this result differs from the Intermediate Disturbance Hypothesis – in which species richness is expected to be the highest at intermediate frequencies of environmental change (Connell 1978) – we recognize that our definitions of "fast", "intermediate" and "low" are arbitrary, as they are in most studies.

One interesting avenue of research would be to explore if species coexistence is maintained in rapidly fluctuating environments. In an extremely fast fluctuating environment, bacteria perceive the environment as a mixture of two carbon sources (Suiter et al. 2003; Bennett et al. 2008). Therefore, we predict that in our system, each species would perceive the environment as a mixture of two carbon sources and would only consume the carbon source in which they grow better (i.e. *A. johnsonii* on benzyl alcohol and *P. putida* on citrate). This specialization on resources is predicted to favor species coexistence (Tilman 1982). A different outcome would be expected in environments changing carbon sources every 50 minutes – equivalent to the doubling times of the species used in this study. We predict that this regime would be detrimental for *A. johnsonii* given that it has a long lag phase of 11 hours when changing from benzyl alcohol to citrate (Table 2). This issue could be addressed using other experimental approaches such as microfluidics.

Overall our findings show that the rate of environmental fluctuations can profoundly impact the ecological dynamics and properties of microbial communities.

Acknowledgments

We thank Søren Molin and Sünje Johanna Pamp for providing the strains. We are grateful to Frederik Hammes and Jürg Sigrist for providing protocols, equipment and facilities to minimize the AOC in our experiments. We also thank Thomas Fleischmann for assistance analyzing samples with HPLC. We thank Colette Bigosch and Kevin Kleeb for technical

assistance. Thanks to the Microbial Systems Ecology group for providing useful feedback during this research. The Swiss National Foundation supported this work. ARV was supported by the European Molecular Biological Organization (EMBO) long-term postdoctoral fellowship (ALTF 241-2015) and the Adaptation to a Changing environment (ACE) postdoctoral fellowship. C.V. was supported by a CASCADE fellowship PCOFUND-GA-2012-600181, by Eawag and ETH.

References

Barabás, G., D'Andrea, R., and Stump, S. M. (2018). Chesson's coexistence theory. *Ecol. Monograph.,* 88, 277-303.

Bennett, M. R., Pang, W. L., Ostroff, N. A., Baumgartner, B. L., Nayak, S., Tsimring, L. S., and Hasty, J. (2008). Metabolic gene regulation in a dynamically changing environment. *Nature,* 454, 1119-1122.

Chesson, P. (2000). Mechanisms of maintenance of species diversity. *Annu. Rev. Ecol. Syst.,* 31, 343-366.

Connell, J. (1978). Diversity in tropical rain forests and coral reefs. *Science,* 199, 1302-1310.

De Roy, K., Marzorati, M., Van den Abbeele, P., Van de Wiele, T., and Boon, N. (2014). Synthetic microbial ecosystems: an exciting tool to understand and apply microbial communities. *Environ. Microbiol.,* 16, 1472-1481.

Dolinšek, J., Goldschmidt, F., and Johnson, D. R. (2016). Synthetic microbial ecology and the dynamic interplay between microbial genotypes. *FEMS Microbiol. Rev.,* 40, 961-979.

Dormand, J. R., and Prince, P. J. (1980). A family of embedded runge-kutta formulae. *J. Comp. Appl. Math,* 6, 19-26.

Faust, K., and Raes, J. (2012). Microbial interactions: from networks to models. *Nat. Rev. Microbiol.,* 10, 538-550.

Fox, J. W. (2013). The intermediate disturbance hypothesis should be abandoned. *Trends Ecol. and Evolut.,* 28, 86-92.

Haagensen, J. A., Hansen, S. K., Christensen, B. B., Pamp, S. J., and Molin, S. (2015). Development of Spatial Distribution Patterns by Biofilm Cells. *Appl. Environ. Microbiol.,* 81, 6120-6128.

Hammes, F. A., and Egli, T. (2005). New method for assimilable organic carbon determination using flow-cytometric enumeration and a natural microbial consortium as inoculum. *Environ. Sci. Technol.,* 39, 3289-3294.

Hanemaaijer, M., Olivier, B. G., Röling, W. F., Bruggeman, F. J., and Teusink, B. (2017). Model-based quantification of metabolic interactions from dynamic microbial-community data. *PLoS One,* 12, e0173183.

Hansen, S. R., and Hubbell, S. P (1980). Single nutrient microbial competition: agreement between experimental and theoretical forecast outcomes. *Science,* 207, 1491-1497.

Hansen, S. K., Haagensen, J. A., Gjermansen, M., Jørgensen, T. M., Tolker-Nielsen, T., and Molin, S. (2007a). Characterization of a Pseudomonas putida rough variant evolved in a mixed-species biofilm with Acinetobacter sp. strain C6. *J. Bacteriol.,* 189, 4932-4943.

Hansen, S. K., Rainey, P. B., Haagensen, J. A. J., and Molin, S. (2007b). Evolution of species interactions in a biofilm community. *Nature,* 445, 533-536.

Hart, S. M., Mi, H., Xie, L., Bello Pineda, J. M., Momeni, B., and Shou, W. (2018). Resolving challenges in quantitative modeling of microbial community dynamics. *bioRxiv*

520 Hoek, T. A., Axelrod, K., Biancalani, T., Yurtsev, E. A., Liu, J., and Gore, J. (2016). Resource
521 availability modulates the cooperative and competitive nature of a microbial cross-feeding
522 mutualism. *PLoS Biol.,* 1002540, 1-17.
523 Jagmann, N., Brachvogel, H. P., and Philipp, B. (2010). Parasitic growth of Pseudomonas
524 aeruginosa in co-culture with the chitinolytic bacterium Aeromonas hydrophila. *Environ.*
525 *Microbiol.,* 12, 1787-1802.
526 Kaas, R. S., Mordhorst, H., Leekitcharoenphon, P., Jensen, J. D., Haagensen, J. A. J., Molin, S.,
527 and Pamp, S. J. (2017). Draft Genome Sequence of Acinetobacter johnsonii C6, an
528 Environmental Isolate Engaging in Interspecific Metabolic Interactions. *Genome. Announc.,*
529 5, e00155-17
530 Lee, I. H., Fredricksen, A. G. and Tsuchiya, H. M. (1976). Dynamics of mixed cultures of
531 Lactobacillus plantarum and Propionibacterium shermaii. *Biotechnol. and Bioeng.,* 18, 513-
532 526.
533 Louca, S., and Doebeli, M. (2015). Calibration and analysis of genome-based models for
534 microbial ecology. *Elife,* 4, e08208.
535 Mackey, R. L., and Currie, D. J. (2001). The diversity-disturbance relationship: is it generally
536 strong and peaked? *Ecology,* 82, 3479-3492.
537 Megee, R. D., Drake, J. F., Fredrickson, A. G., and Tsuchiya, H. M. (1972). Studies in
538 intermicrobial symbiosis. Saccharomyces cerevisiae and Lactobacillus casei. *Can. J.*
539 *Microbiol.,* 18, 1733-1742.
540 Miller, A. D., Roxburgh, S. H., and Shea, K. (2011). How frequency and intensity shape
541 diversity-disturbance relationships. *Proc. Natl. Acad. Sci. USA,* 108, 5643-5648.
542 Monod, J. (1942). Recherches sur la croissance des cultures bactériennes. Hermann et ci,
543 Paris, 1-210.

544 Shampine, L. F., and Reichelt, M. W. (1997). The MATLAB ODE Suite. *Siam J. Sci. Comput.,*
545 18, 1-22.
546 Suiter, A. M., Bänziger, O., and Dean, A. M. (2003). Fitness consequences of a regulatory
547 polymorphism in a seasonal environment. *Proc. Natl. Acad. Sci. USA,* 100, 12782-12786.
548 Tilman, D. 1982. Resource competition and community structure. Princeton Univ. Press,
549 Princeton, NJ, 1-296.
550 Turkarslan, S., Raman, A. V., Thompson, A. W., Arens, C. E., Gillespie, M. A., von Netzer,F. *et*
551 *al.* (2017). Mechanism for microbial population collapse in a fluctuating resource
552 environment. *Mol. Syst. Biol.,* 13, 919.
553 Vasi, F., Travisano, M., and Lenski, R. E. (1994). Long-term experimental evolution in
554 Escherichia coli II. Changes in life-history traits during adaptation to a seasonal environment.
555 *Am. Nat.,* 144, 432-456.
556 Vorholt, J. A. (2012). Microbial life in the phyllosphere. *Nat. Rev. Microbiol.,* 10, 828-840.
557 Yi, X., and Dean, A. M. (2013). Bounded population sizes, fluctuating selection and the
558 tempo and mode of coexistence. *Proc. Natl. Acad. Sci. USA,* 110, 16945-16950.
559
560 **Figures and tables**

561 **Figure Legends**

562 **Fig 1. Species have different interactions depending on the carbon source provided.**
563 Species have an exploitative interaction in benzyl alcohol (A) and a competitive interaction
564 in citrate (B). Population density trajectories of monocultures (left panel) and co-cultures
565 (right panel), estimated from CFU/ml after six daily serial transfers (100-fold dilution). Each
566 line corresponds to a local polynomial regression fitting of three replicates with 95%

confidence interval. Graphs were constructed with the function stat_smoot (R version 3.2.3).

Fig 2. Mathematical model predicts different ecological outcomes depending on the frequency of environmental change. The results derived from the mathematical model are plotted when simulating regimes that fluctuate between the two carbon sources daily or every two, three, four and five days. We used the parameters in Table 2 to run the model and the results (in OD units) were converted to cell densities (in CFU/ml) using the conversion rates $4*10^9$ CFU/ml for *A. johnsonii* and $4*10^8$ CFU/ml for *P. putida*. Each line corresponds to the connection between the final densities of each species after daily cycles of growth. In high-frequency regimes, the two species coexist, while in low-frequency regimes both species go extinct.

Fig 3. Experiments in co-cultures validate theoretical predictions. Population density (CFU/ml) trajectories of co-cultures are shown over six days of serial transfers (100-fold dilution) in five fluctuating regimes. In the 4 days fluctuating regime, the population of *A. johnsonii* that did not went extinct is represented with diamonds. Each line corresponds to a local polynomial regression fitting of three replicates with 95% confidence interval. Graphs were constructed with the function stat_smoot (R version 3.2.3).

Tables.

Table 1. Mathematical model

Bacterial growth	
A. johnsonii:	$\frac{dA}{dt} = \mu_{maxA} A \left(\frac{Boh}{k_{BohA} + Boh} + \frac{Ben}{k_{BenA} + Ben} + \frac{Ci}{k_{CiA} + Ci}\right)$
P. putida:	$\frac{dP}{dt} = \mu_{maxP} P \left(\frac{Ben}{k_{BenP} + Ben} + \frac{Ci}{k_{CiP} + Ci}\right)$
Resource changes	
Benzyl alcohol	$\frac{dBoh}{dt} = -\left(\frac{V_{BohA} Boh}{k_{BohA} + Boh} A\right)$
Benzoate	$\frac{dBen}{dt} = -\left(\frac{V_{BenA} Ben}{k_{BenA} + Ben} A + \frac{V_{BenP} Ben}{k_{BenP} + Ben} P\right) + \left(\frac{V_{BohA} Boh}{k_{BohA} + Boh} A\right) . \alpha$
Citrate	$\frac{dCi}{dt} = -Ci\left(\frac{V_{CiA} Ci}{k_{CiA} + Ci} A + \frac{V_{CiP} Ci}{k_{CiP} + Ci} P\right)$

Variables		Unit
A	Density of *A. johnsonii*	unitless (OD)
P	Density of *P. putida*	unitless (OD)
Boh	Concentration of benzyl alcohol in culture	mM
Ben	Concentration of benzoate in culture	mM
Ci	Concentration of citrate in culture	mM
Parameters		**Unit**
μ_{maxA}	Maximum growth rate of *A. johnsonii*	h^{-1}
μ_{maxP}	Maximum growth rate of *P.putida*	h^{-1}
k_{BohA}	Half-saturation constant describing saturation of benzyl alcohol for *A. johnsonii* growth	mM
k_{BenA}	Half-saturation constant describing saturation of benzoate for *A. johnsonii* growth	mM
k_{BenP}	Half-saturation constant describing saturation of benzoate for *P. putida* growth	mM
k_{CiA}	Half-saturation constant describing saturation of citrate for *A. johnsonii* growth	mM
k_{CiP}	Half-saturation constant describing saturation of citrate for *P. putida* growth	mM
V_{BohA}	Maximum uptake rate	mM/unitless(OD)/h
V_{BenA}	Maximum uptake rate	mM/unitless(OD)/h
V_{BenP}	Maximum uptake rate	mM/unitless(OD)/h
V_{CiA}	Maximum uptake rate	mM/unitless(OD)/h
V_{CiP}	Maximum uptake rate	mM/unitless(OD)/h
α	Excretion rate proportionality factor	dimensionless

Table 2. Parameters' values used in the model

Description	Parameter estimated (SE)[1]
Growth on Benzyl Alcohol	μ_{maxA} = 0.54 (0.07) k_{BohA} = 0.12 (0.03) V_{BohA} =11.20 (2.63)
Growth on Benzoate	μ_{maxA} = 0.58 (0.06) k_{BenA} = 0.13 (0.01) V_{BenA} =8.03 (0.62) μ_{maxP} = 0.76 (0.01) k_{BenP} = 0.03 (0.01) V_{BenP} = 19.22 (0.44)
Growth on Citrate	μ_{maxA} = 0.25 (0.04) k_{CiA}= 0.72 (0.12) V_{CiA} = 7.98 (1.13) μ_{maxP} = 1.01(0.10) k_{CiP} = 0.36 (0.03) V_{CiP} = 48.50 (0.30)
Excretion rate proportionality factor	α = 0.51
Duration of lag phase (h^{-1}) when diluting a saturated culture into a fresh medium	
From Benzyl alcohol to Benzyl alcohol	λ_A= 0 λ_P= 0
From Benzyl alcohol (or Benzoate) to Citrate	λ_A= 11.6 (1.0) λ_P= 0
From Citrate to Citrate	λ_A= 0 λ_P= 0
From Citrate to Benzyl Alcohol (or Benzoate)	λ_A= 0.4 (0.4) λ_P= 0

[1]The mean and standard error (SE) were calculated from 3 replicate growth curves (see Fig. S4).

Supporting Information

Fig. S1. Procedure followed to estimate the maximum uptake rates and the half-saturation constants. We used the OD growth curves data shown in plot 1) to estimate the maximum uptake rate and the half-saturation constant. Given that we did not measure

593 experimentally the changes in resources, we used a multi-step approach to model the
594 changes in resources and the uptake rate from the growth curves. The dots correspond to
595 the OD measurements acquired every 5 minutes (background subtracted) for *P. putida*
596 grown in 1 mM citrate (only one of the three replicate growth curves is shown; all the
597 replicates are shown in Fig. S4). The detection limit of the plate reader is represented by a
598 grey line. The red line corresponds to the data used for the analyses which were smoothed
599 with the smooth function of Matlab (version R2017a, Mathworks), using a moving average
600 filter of one hour. We used these OD data to estimate the final yield and to estimate the
601 instantaneous growth rate shown in plot 2). Assuming that the yield is constant, we
602 modeled the change in resources concentration (plot 3) and the change in the uptake rate
603 (plot 4). Finally, we plotted the uptake rate as a function of the resources concentration
604 (plot 5) and fitted the maximum uptake rate (V) and the half-saturation constant (K) to the
605 part of the data that had a low error variance (based on visual inspection; the data in the
606 grey rectangle were not included for the fitting).
607
608 **Fig. S2. Data used to convert the OD values to cell density values.** We used saturated
609 cultures of *A. johnsonii* and *P. putida* grown in benzoate (1 mM) to relate the cell density
610 (CFU/ml) to the optical density values. We fitted a linear relationship between the OD and
611 the cell density (CFU/ml) and set the intercept to 0. The conversion rates for *A. johnsonii*
612 and *P. putida* were $4*10^9$ and $4*10^8$ CFU/ml, respectively.
613
614 **Fig. S3. Population densities of monocultures when no carbon was added to the medium**
615 **(i.e. control environment).** Population density trajectories of monocultures of *A. johnsonii*
616 and *P. putida*, estimated from CFU after six daily serial transfers (100-fold dilution). Each line

corresponds to a local polynomial regression fitting of three replicates with 95% confidence interval. Graphs were constructed with the function stat_smoot (R version 3.2.3).

Fig. S4. Growth curves used to estimate different parameters for the mathematical model. We show all the growth curves used to parameterize the mathematical model. The four panels correspond to the plots 1,2, 3 and 5 presented in Fig. S1 (upper-left panel corresponds to plot 1 of Fig. S1; upper-right panel corresponds to plot 2 of Fig. S1; lower-left panel corresponds to plot 3 of Fig. S1; lower-right panel corresponds to plot 5 of Fig. S1). The three different colors in each panel correspond to three replicate growth curves. The shaded areas in the bottom-right panels correspond to the part of the data with a high error variance (based on visual inspection) that were not used for the fitting of the maximum uptake rate (V) and the half-saturation constant (K). In some cases, the part of the data with high error variance varied between replicates (i.e. replicates varied in the duration of the lag phase); in those cases, we highlighted the part that we excluded for the fitting with different colors, each corresponding to the color of the respective replicate. We fitted the parameters to each growth curve individually and used the average of three replicates to parameterize the model. In addition, we show the r^2 value for each fit in the bottom-right panel.

Fig. S5. *A. johnsonii* consumes benzyl alcohol and excretes benzoate into the medium. At the beginning of a 22 hours growth cycle, *A. johnsonii* consumes benzyl alcohol while excreting benzoate into the medium. When *A. johnsonii* exhaust the benzyl alcohol, around 12 hours, it consumes the benzoate previously excreted (i.e. the benzoate disappears from the supernatant after 13 hours). A). Changes in the concentrations of benzyl alcohol and benzoate in the supernatant of three independent monocultures of *A. johnsonii* (replicates)

641 measured by HPLC over 22 hours. B). Log-transformed concentrations of metabolites in
642 time. The values plotted for benzyl alcohol correspond to the log-transformed
643 concentrations minus the mean initial concentrations of benzyl alcohol (0.595 mM),
644 multiplied by zero. C). *A. johnsonii* growth of three independent monocultures in benzyl
645 alcohol (0.6 mM). The supernatant of these cultures was used to measure the metabolites
646 concentrations shown in panel A.
647
648 **Fig. S6. Results obtained from the mathematical model when simulating co-cultures in a**
649 **single resource.** Growth on benzyl alcohol is simulated in the left panel and growth on
650 citrate is simulated in the right panel. We used the parameters in Table 2 to run the model
651 and the results (in OD units) were converted to cell densities (in CFU/ml) using the
652 conversion rates $4*10^9$ CFU/ml for *A. johnsonii* and $4*10^8$ CFU/ml for *P. putida*. The thin
653 lines show the simulated growth over 24 hours. Each tick line corresponds to the connection
654 between the final densities of each species after daily cycles of growth.
655
656 **Fig. S7. Results obtained from the mathematical model and from experiments for a six-**
657 **days fluctuating regime.** The model predicts that both *A. johnsonii* and *P. putida* get extinct
658 in a 6-days fluctuating regime. Experiments for one replicate show that only A. *johnsonii* get
659 extinct while *P. putida* persist at low densities in benzyl alcohol and recover when the
660 carbon source change back to citrate. The light-colored dots connected by lines show the
661 results from the model when simulating co-cultures in a 6-days fluctuating regime. The lines
662 connect the final density of each species after a daily cycle of growth. The dark-colored dots
663 show the population density trajectories of a co-culture of *A. johnsonii* and *P. putida*,
664 estimated from CFU/ml after eighteen daily serial transfers.

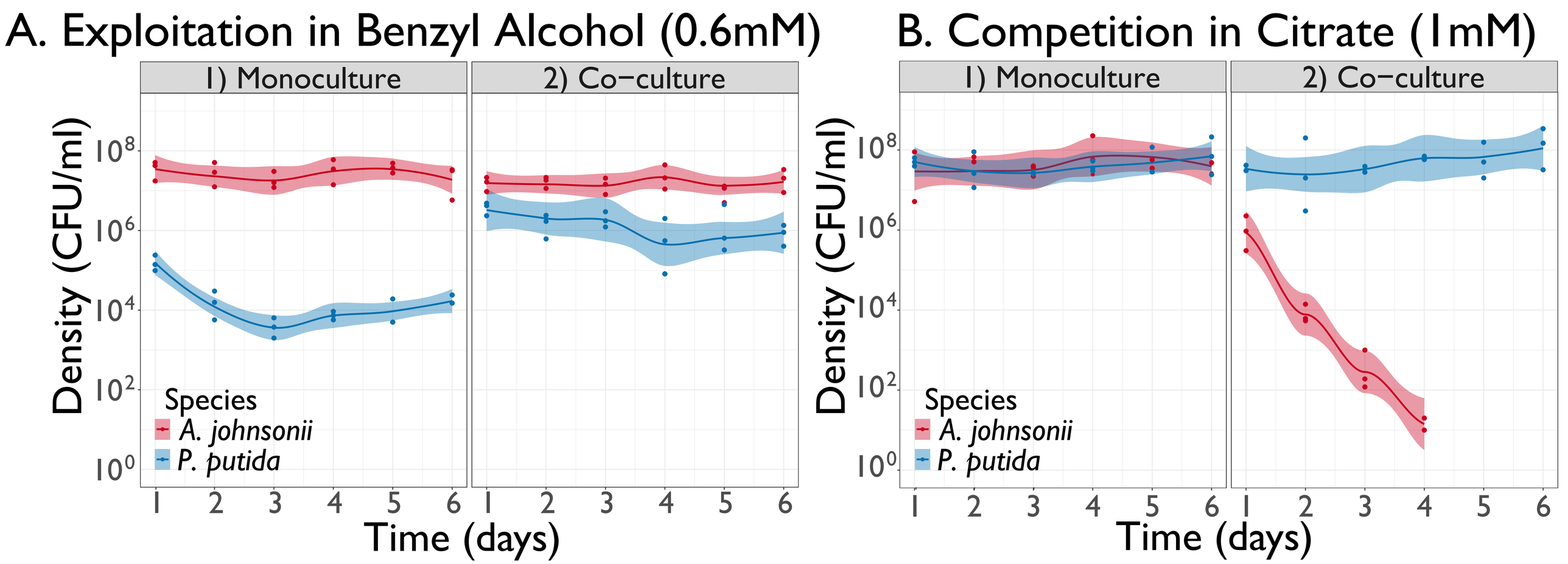
A. Exploitation in Benzyl Alcohol (0.6mM)
B. Competition in Citrate (1mM)
1) Monoculture
2) Co−culture
Density (CFU/ml)
10^8
10^6
10^4
10^2
10^0
Species
A. johnsonii
P. putida
1
2
3
4
5
6
Time (days)

1 day fluctuations

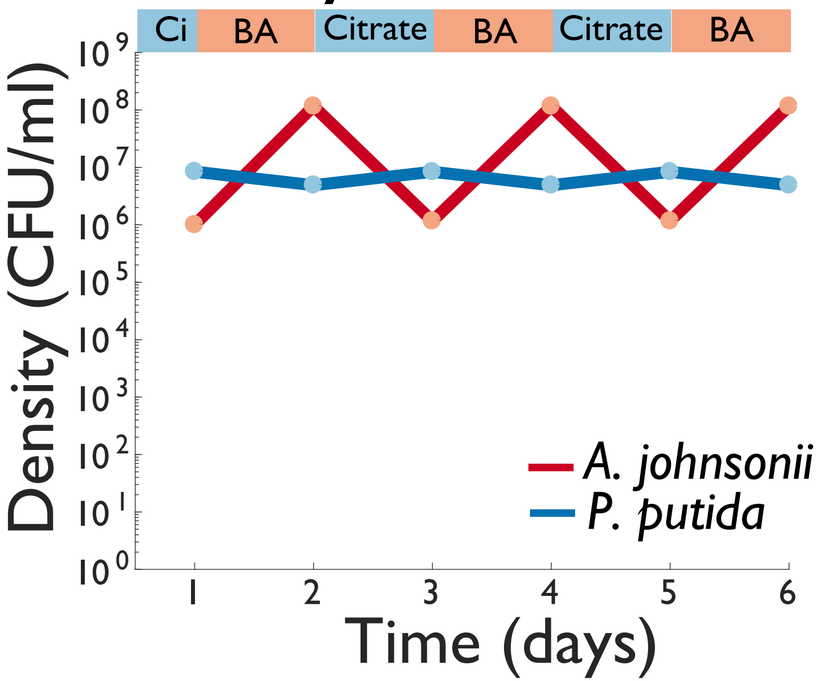

2 days fluctuations

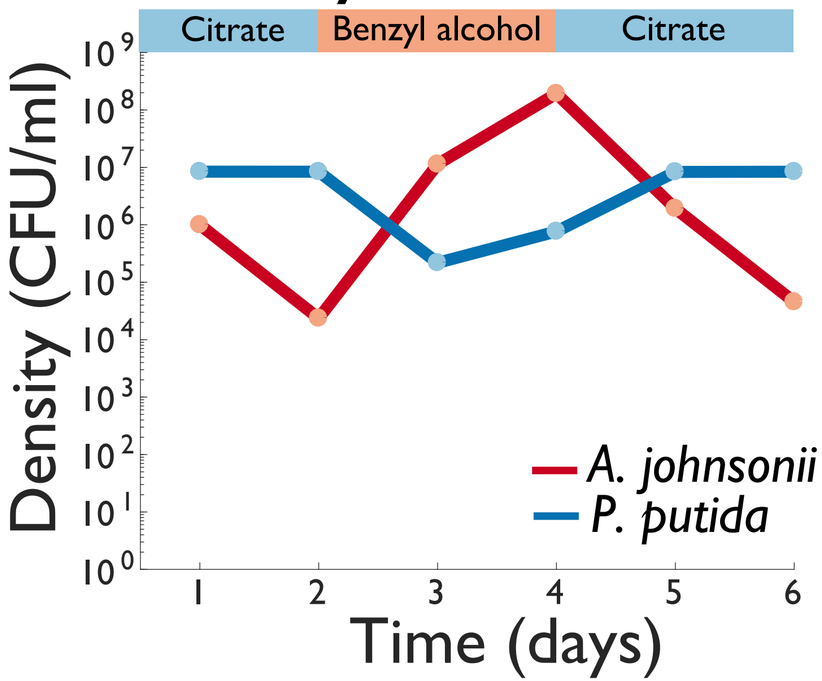

3 days fluctuations

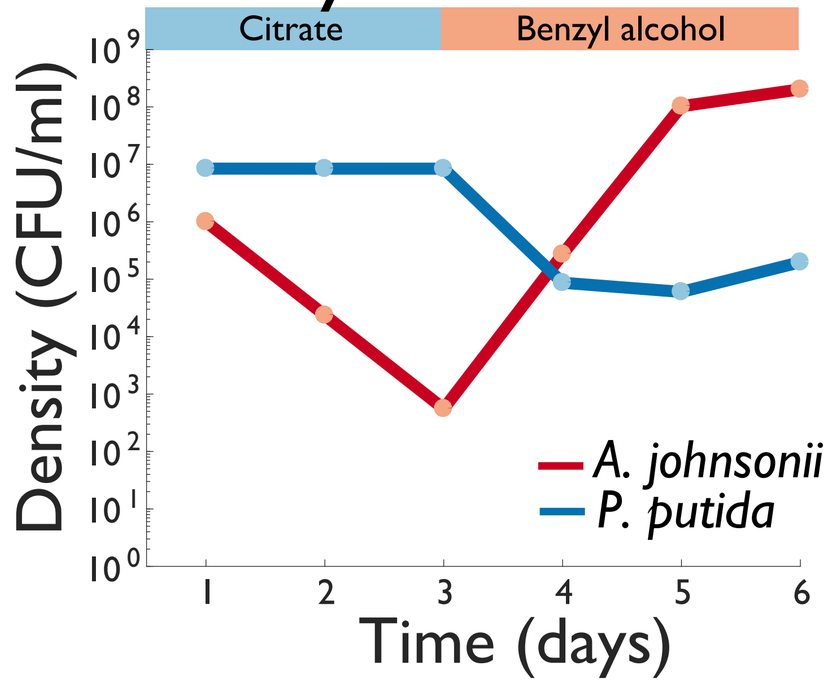

4 days fluctuations

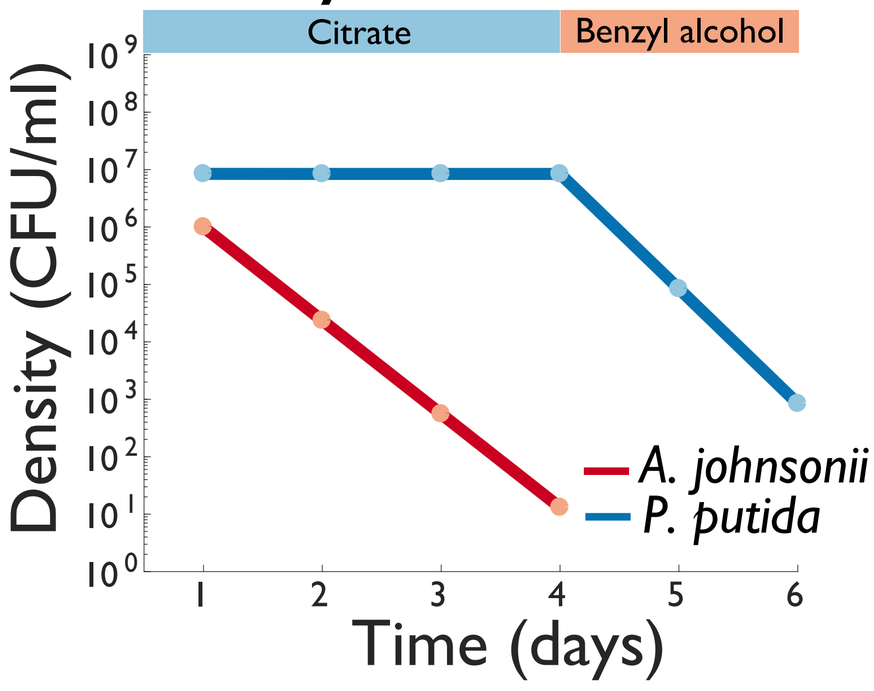

5 days fluctuations

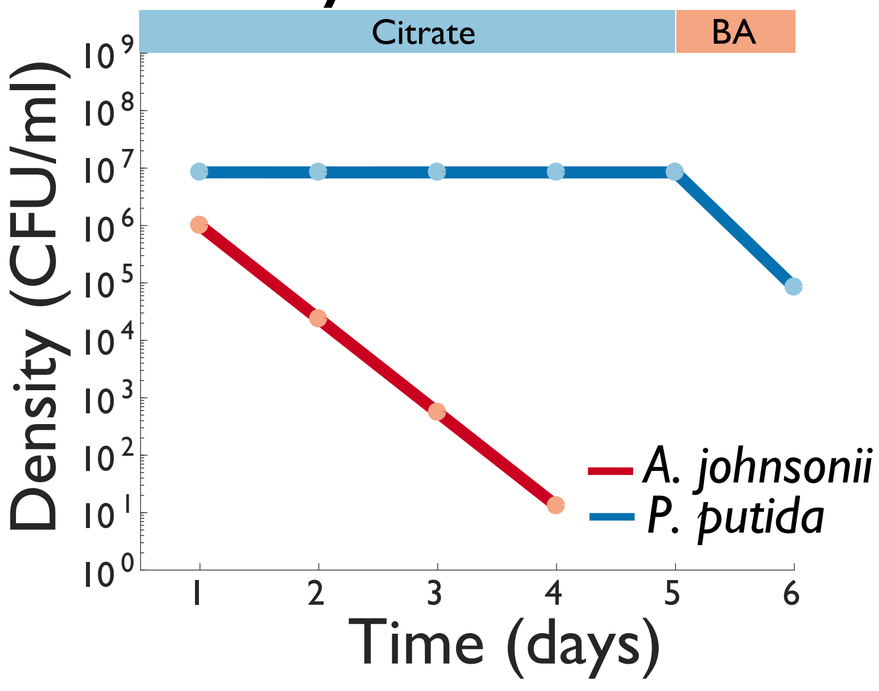

1 day fluctuations

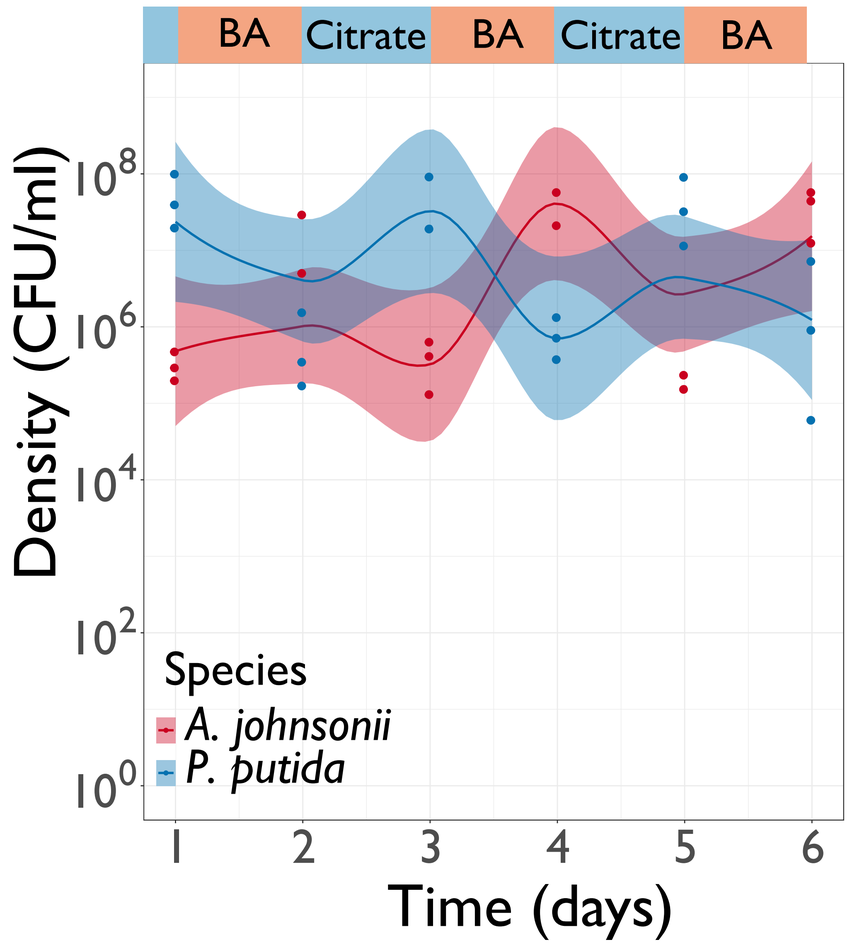

2 days fluctuations

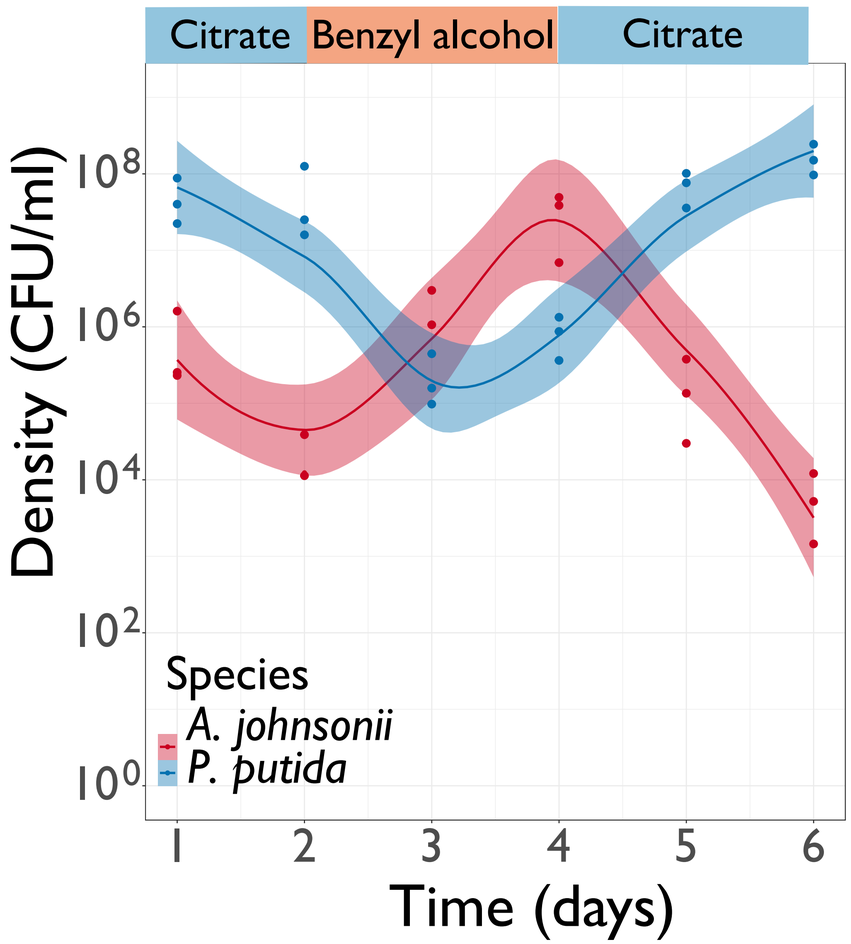

3 days fluctuations

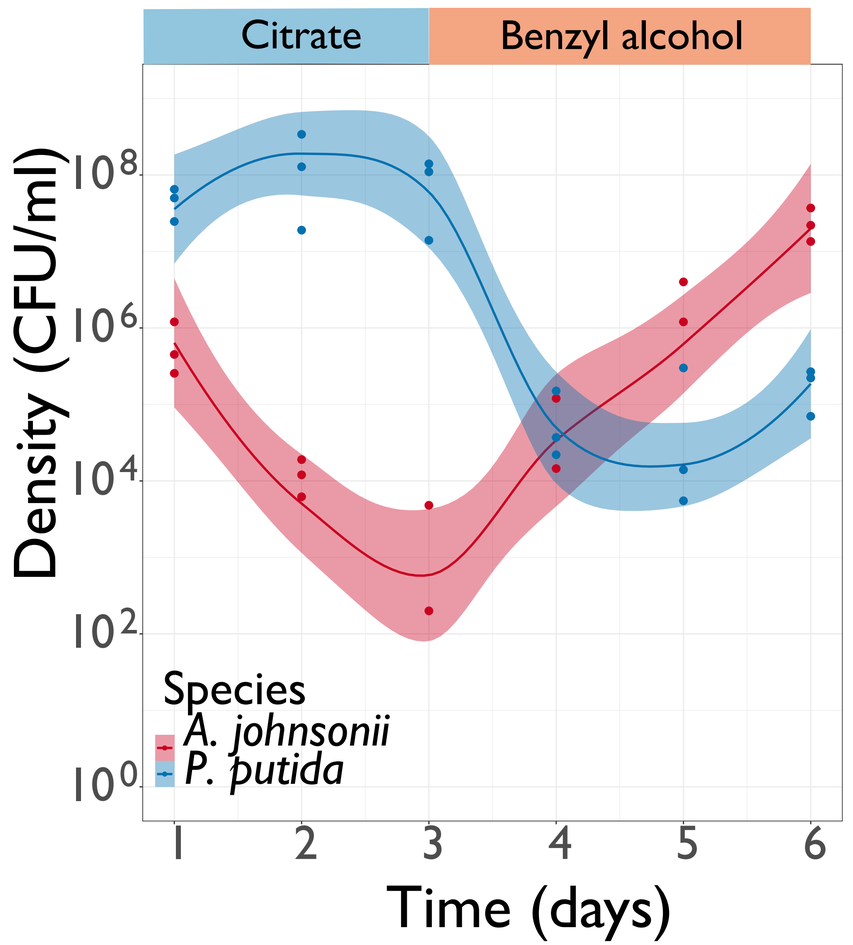

4 days fluctuations

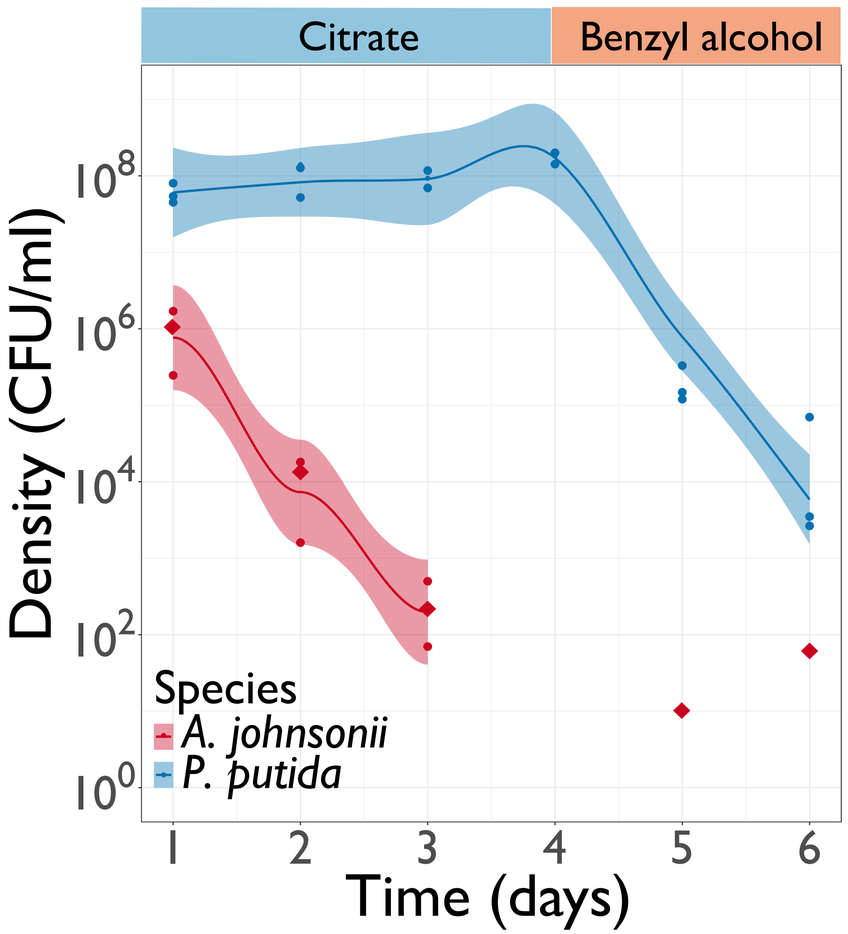

5 days fluctuations

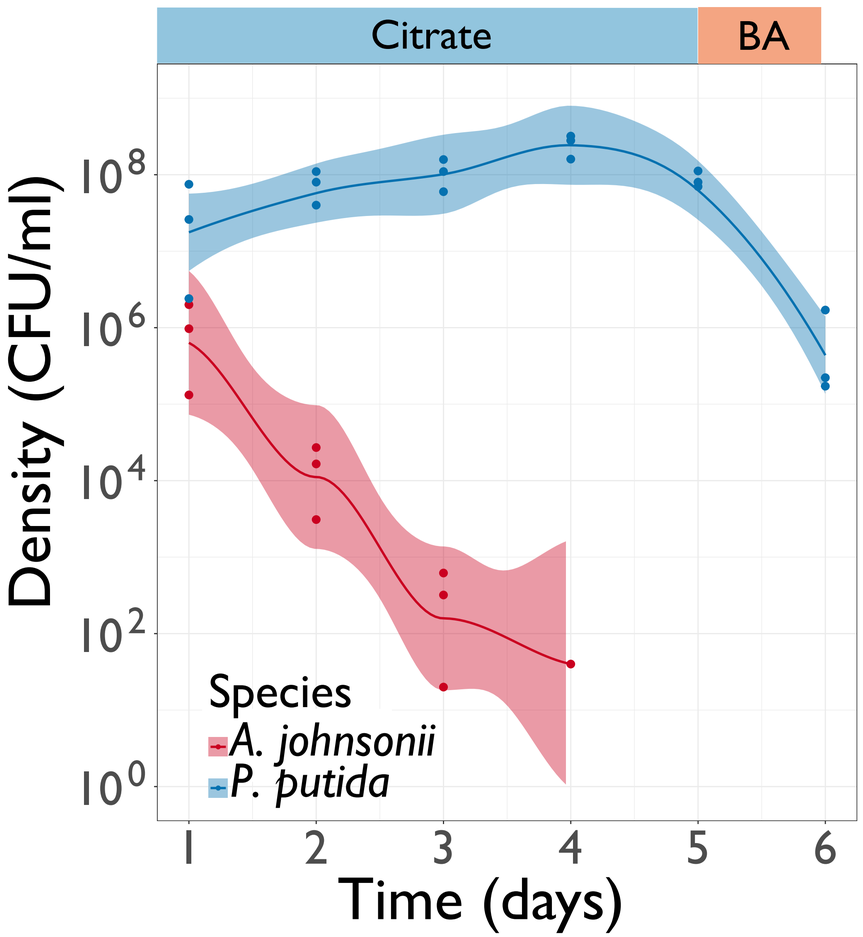

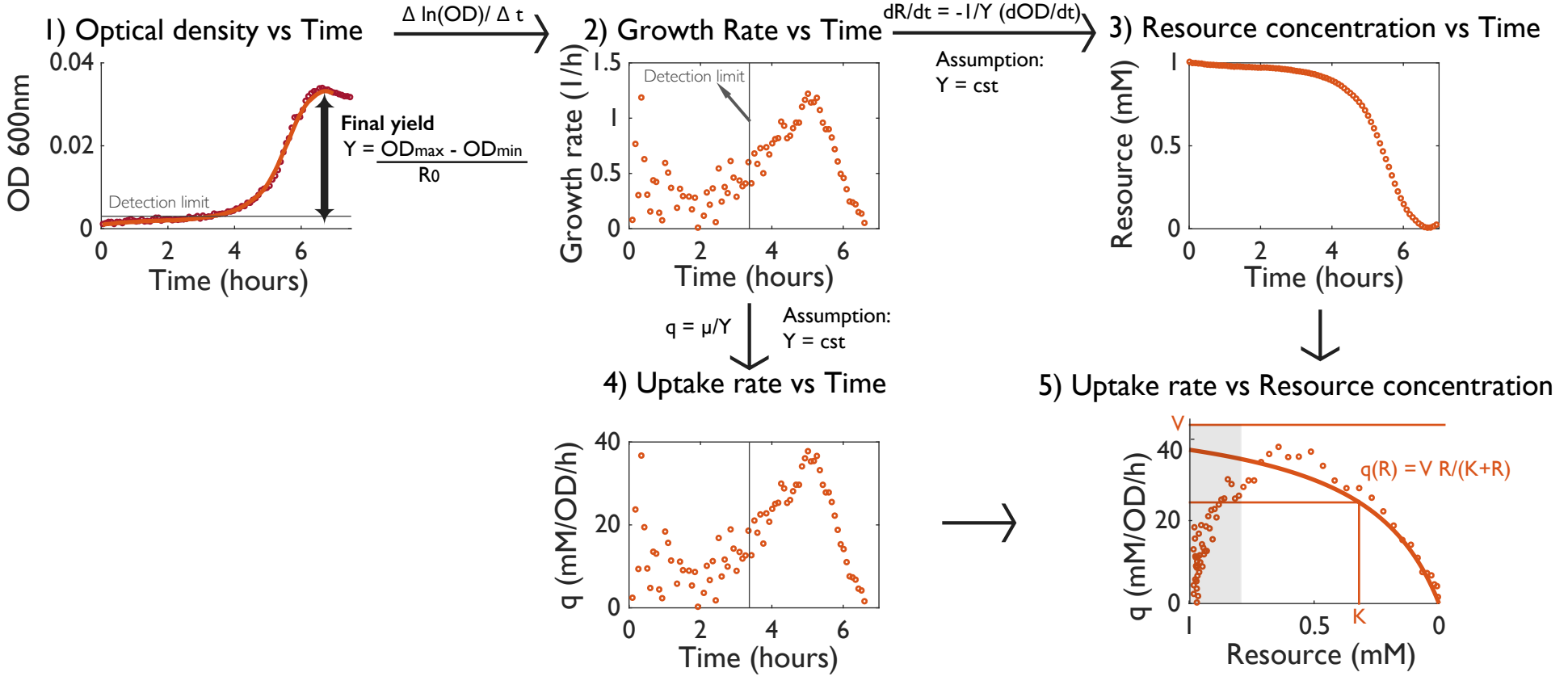
1) Optical density vs Time
OD 600nm
0.04
0.02
0
Detection limit
0
2
4
6
Time (hours)
Final yield
Y = ODmax - ODmin / R0
Δ ln(OD)/ Δ t
2) Growth Rate vs Time
Growth rate (1/h)
1.5
1
0.5
0
Detection limit
Time (hours)
dR/dt = -1/Y (dOD/dt)
Assumption:
Y = cst
3) Resource concentration vs Time
Resource (mM)
1
0.5
0
Time (hours)
q = μ/Y
Assumption:
Y = cst
4) Uptake rate vs Time
q (mM/OD/h)
40
20
0
Time (hours)
5) Uptake rate vs Resource concentration
V
q(R) = V R/(K+R)
K
Resource (mM)

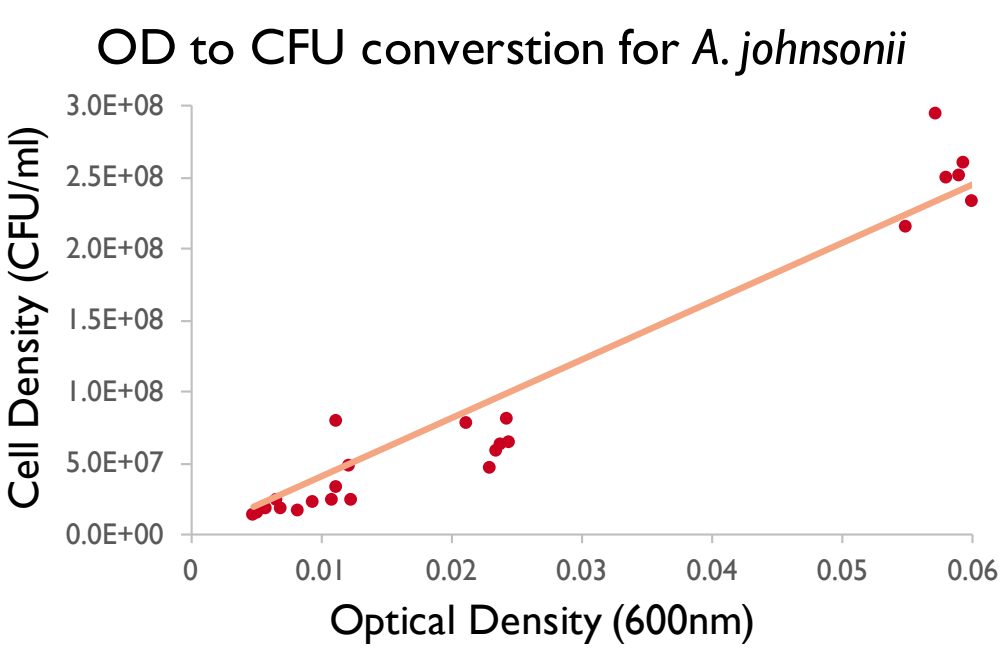
OD to CFU converstion for A. johnsonii
Cell Density (CFU/ml)
3.0E+08
2.5E+08
2.0E+08
1.5E+08
1.0E+08
5.0E+07
0.0E+00
0
0.01
0.02
0.03
0.04
0.05
0.06
Optical Density (600nm)

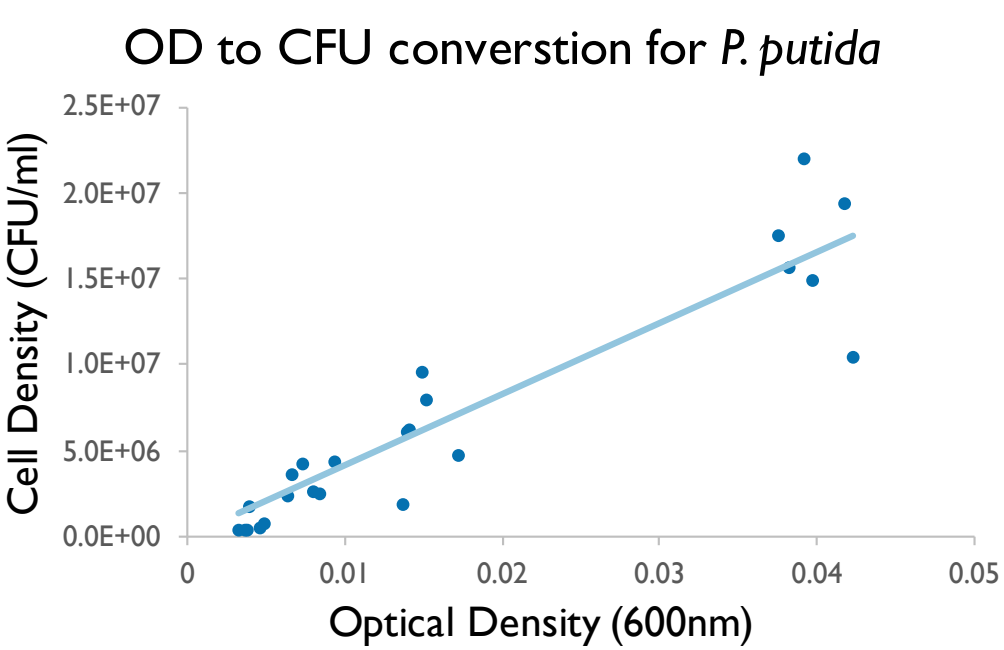
OD to CFU converstion for P. putida
Cell Density (CFU/ml)
2.5E+07
2.0E+07
1.5E+07
1.0E+07
5.0E+06
0.0E+00
0
0.01
0.02
0.03
0.04
0.05
Optical Density (600nm)

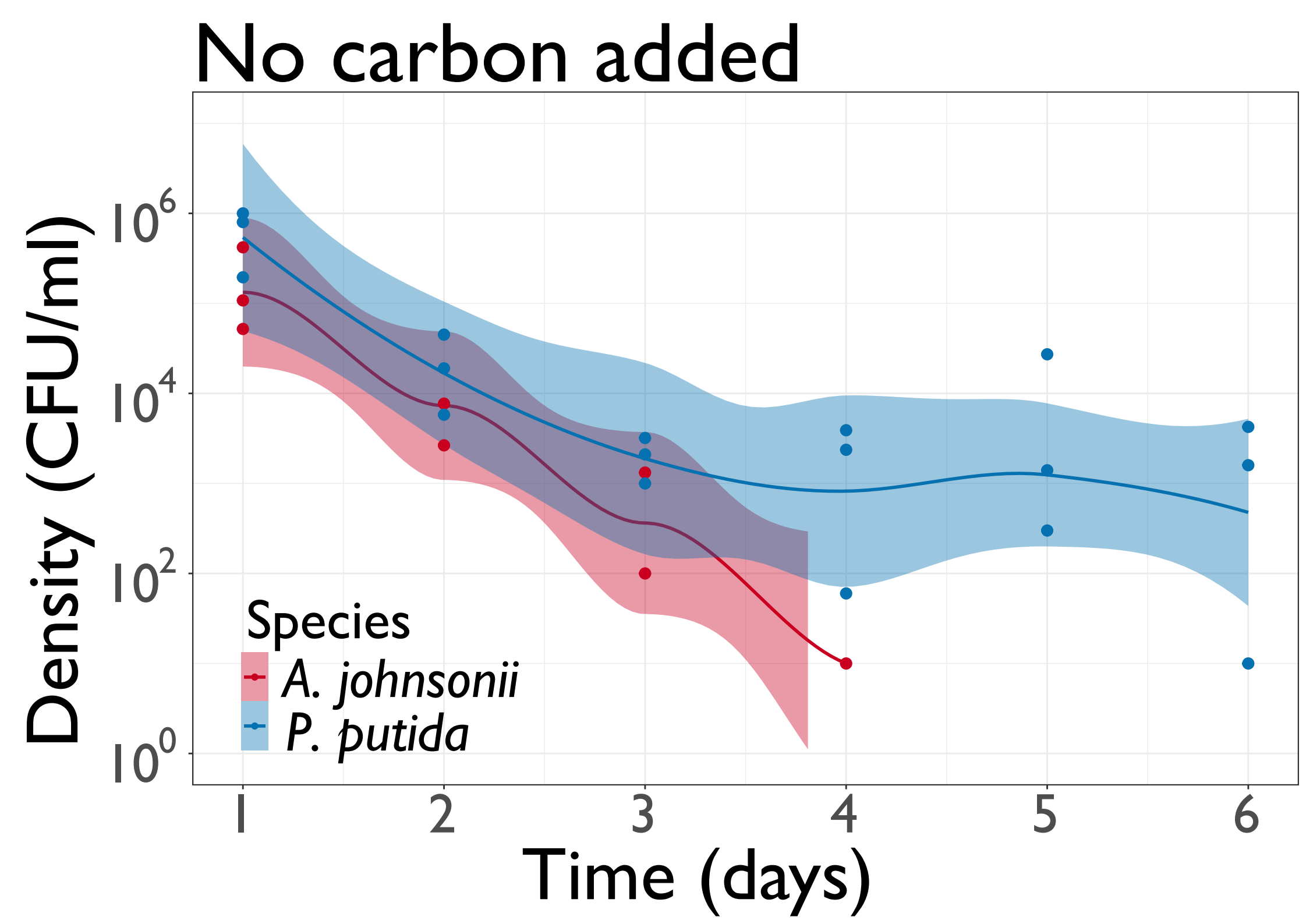
No carbon added
Density (CFU/ml)
10^6
10^4
10^2
10^0
1
2
3
4
5
6
Time (days)
Species
A. johnsonii
P. putida

A. johnsonii in Benzyl alcohol (0.6mM)

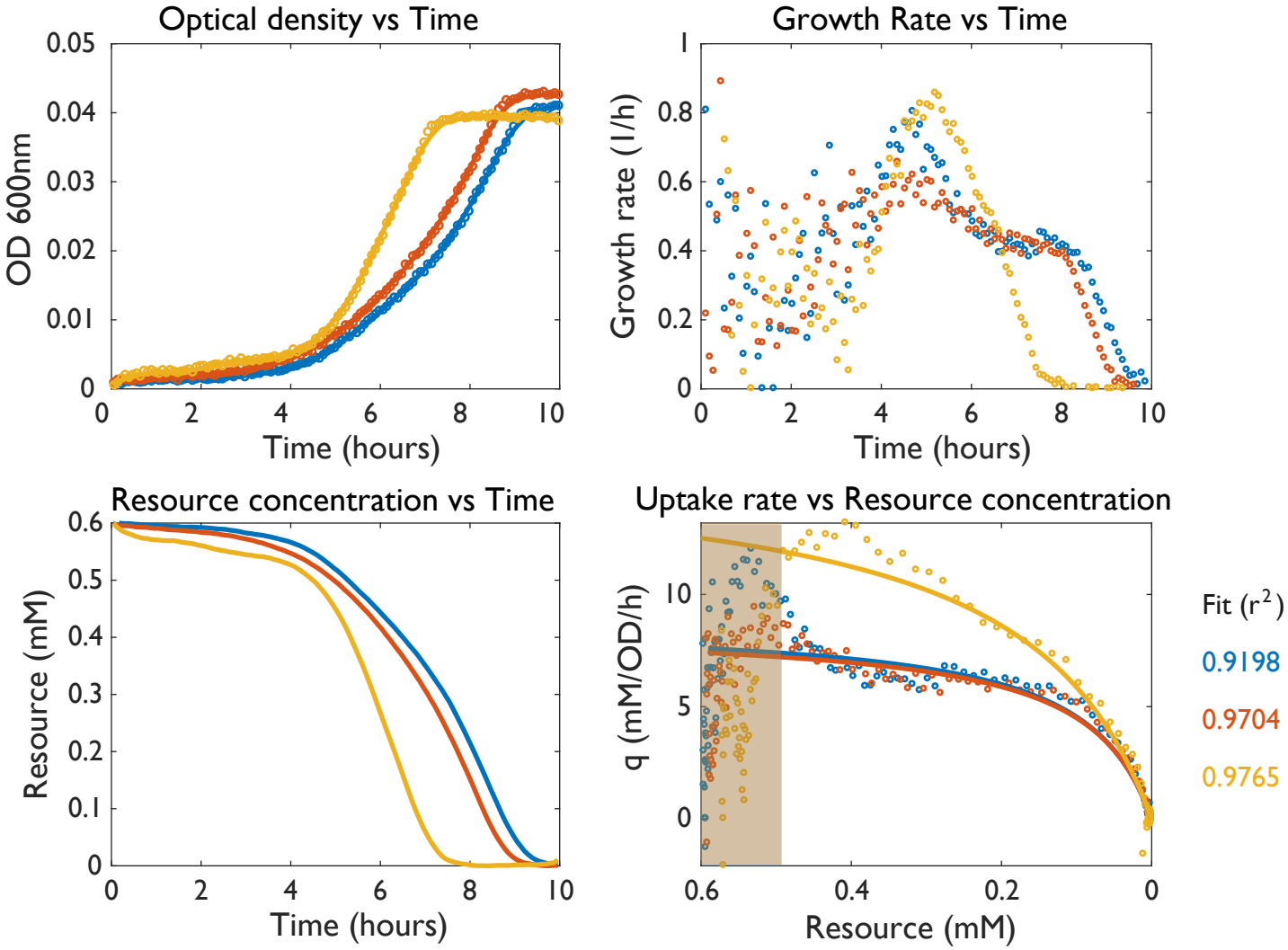

A. johnsonii in Benzoate (1mM)

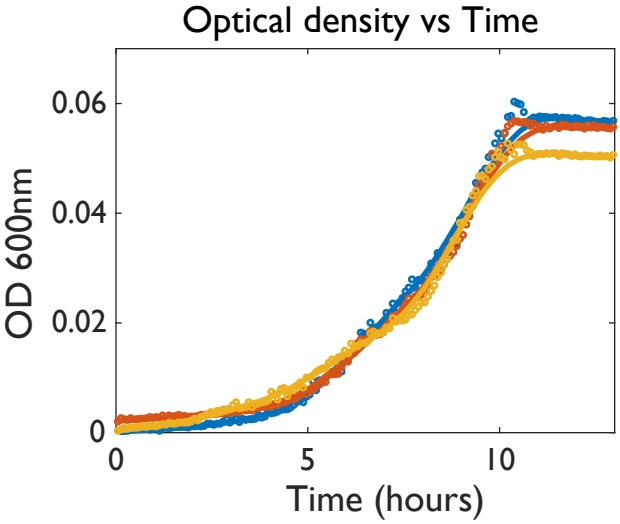

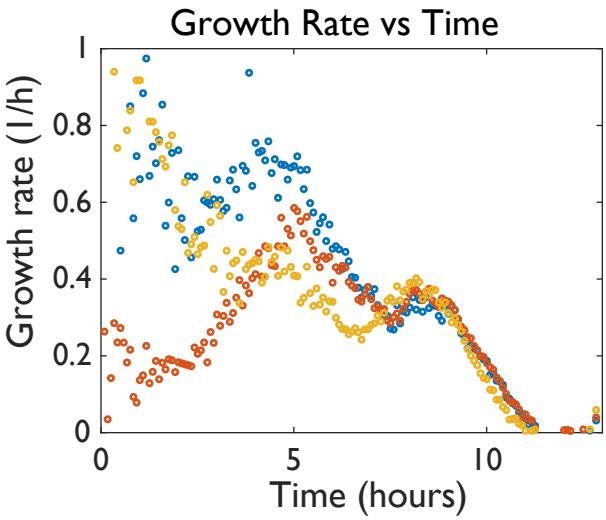

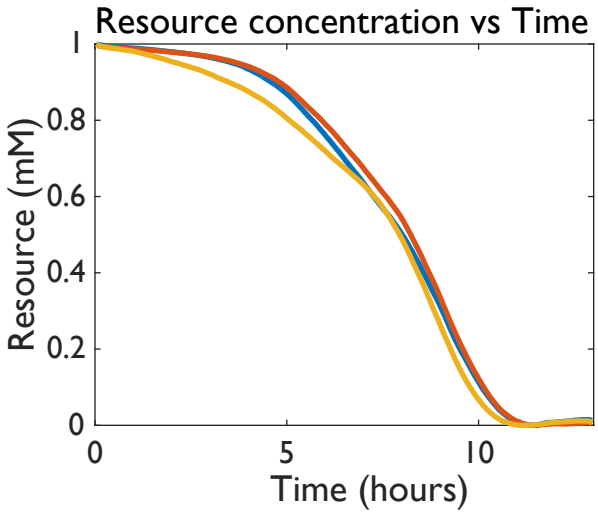

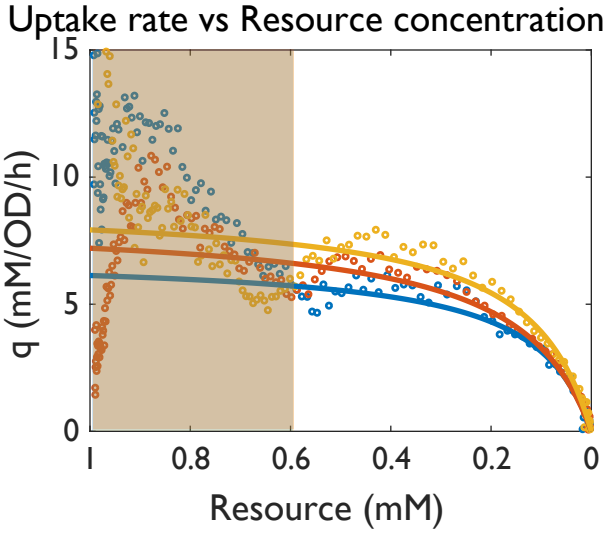

P. putida in Benzoate (1mM)

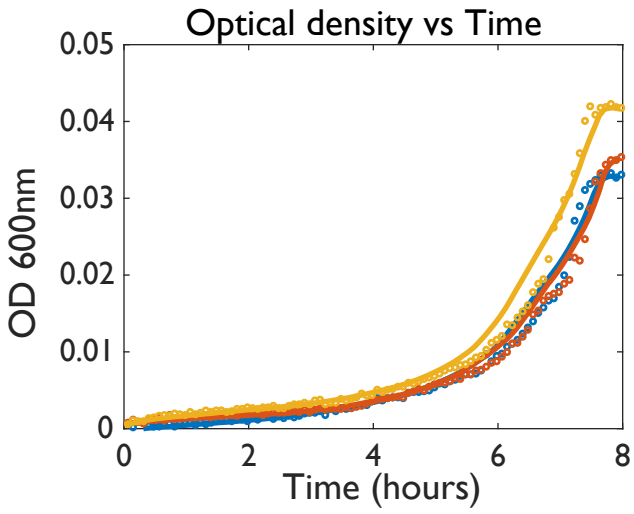

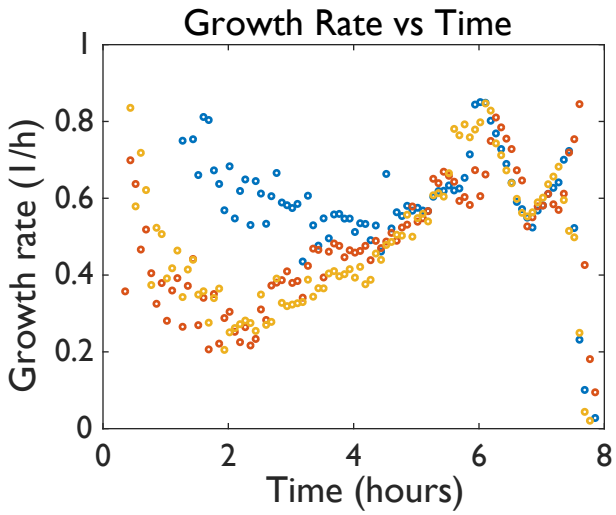

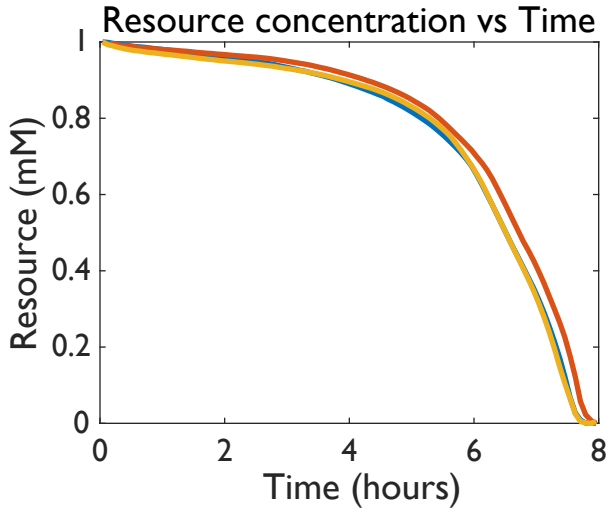

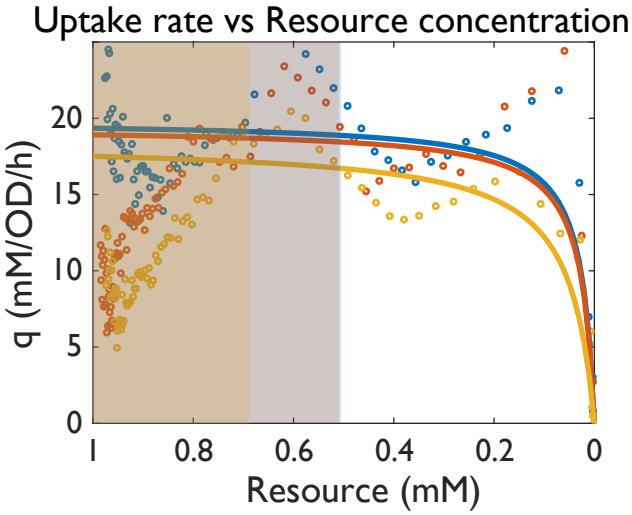

A. johnsonii in Citrate (1mM)

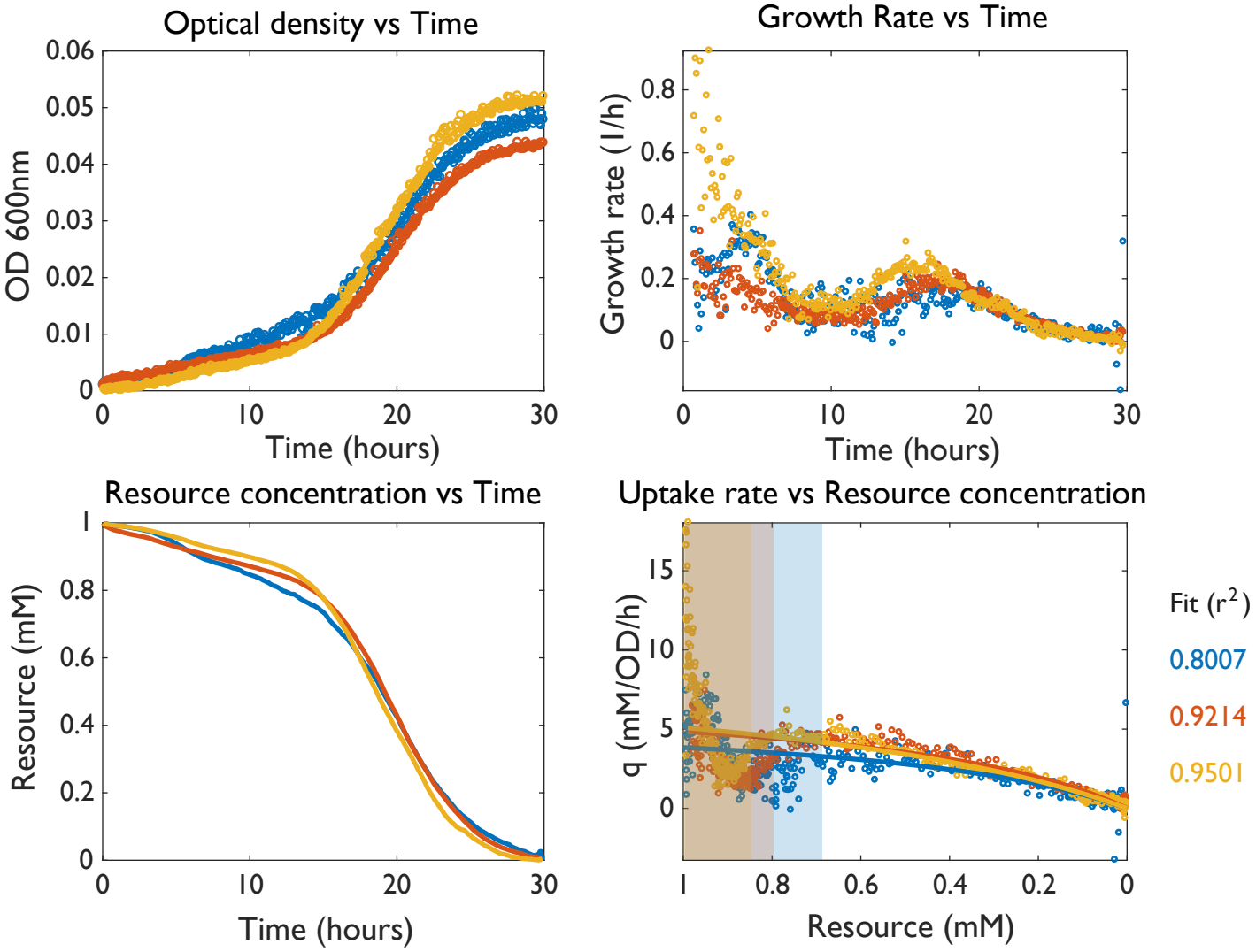

P. putida in Citrate (1mM)

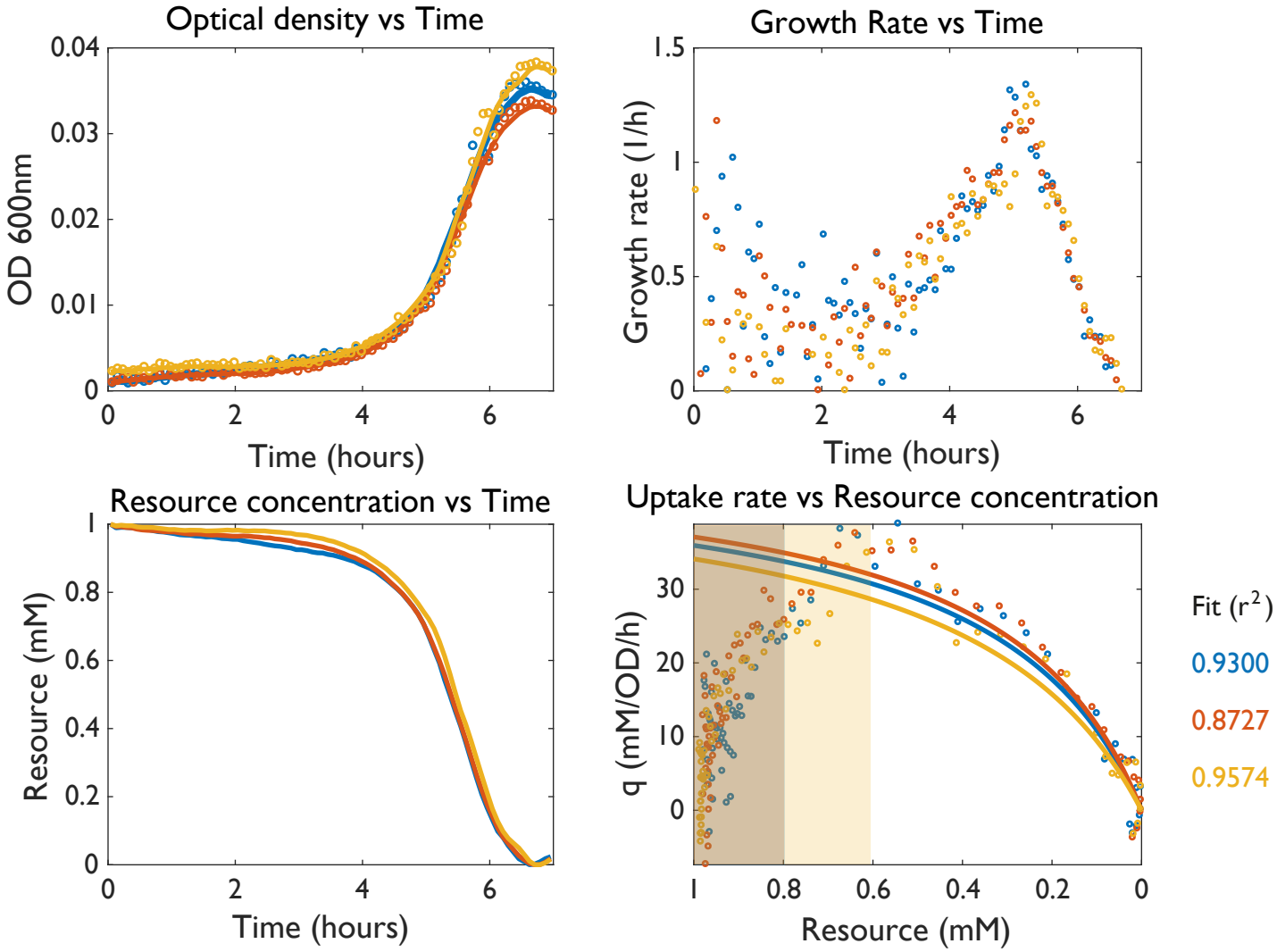

A

Metabolites changes

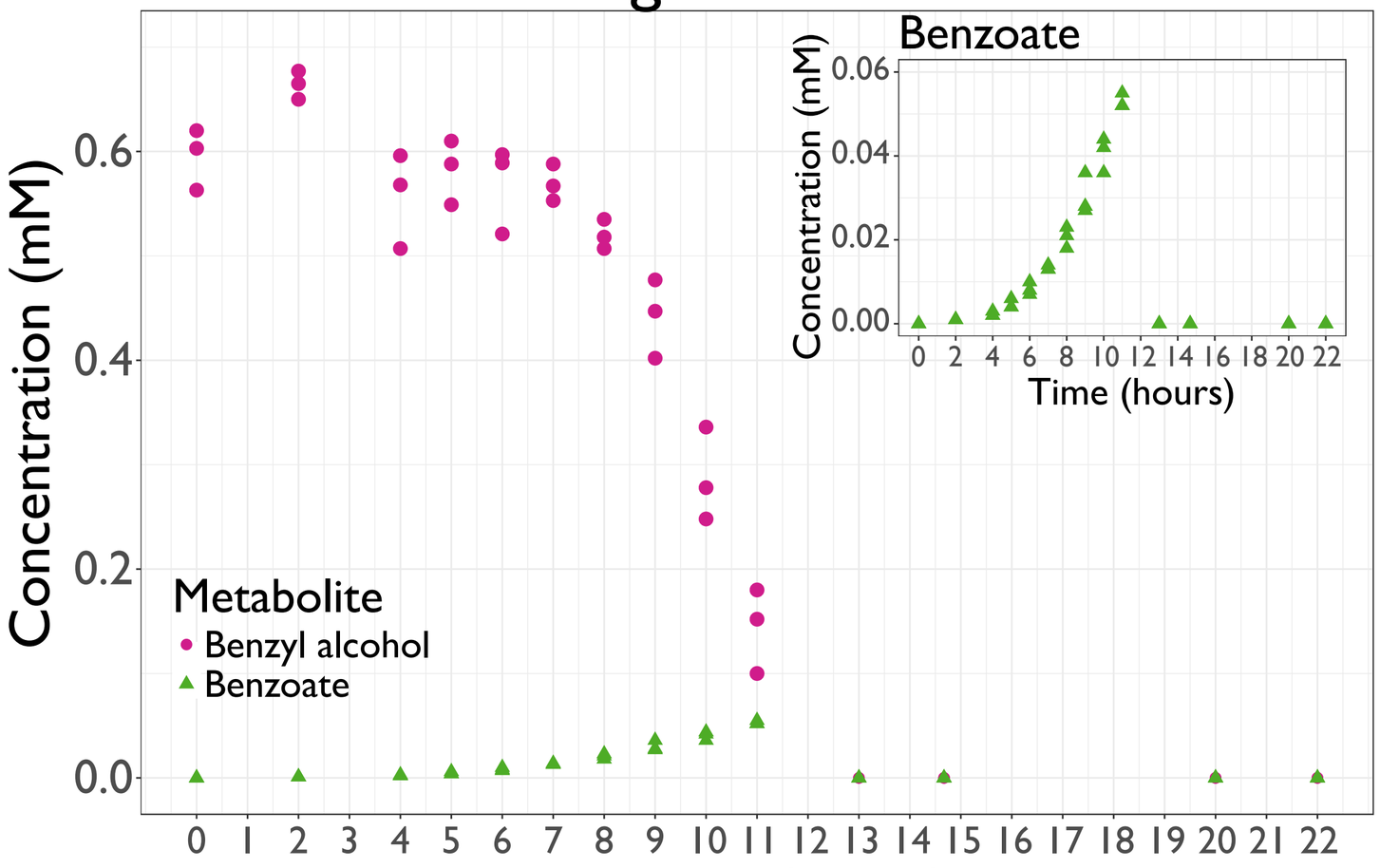

B

Consumption and excretion rates

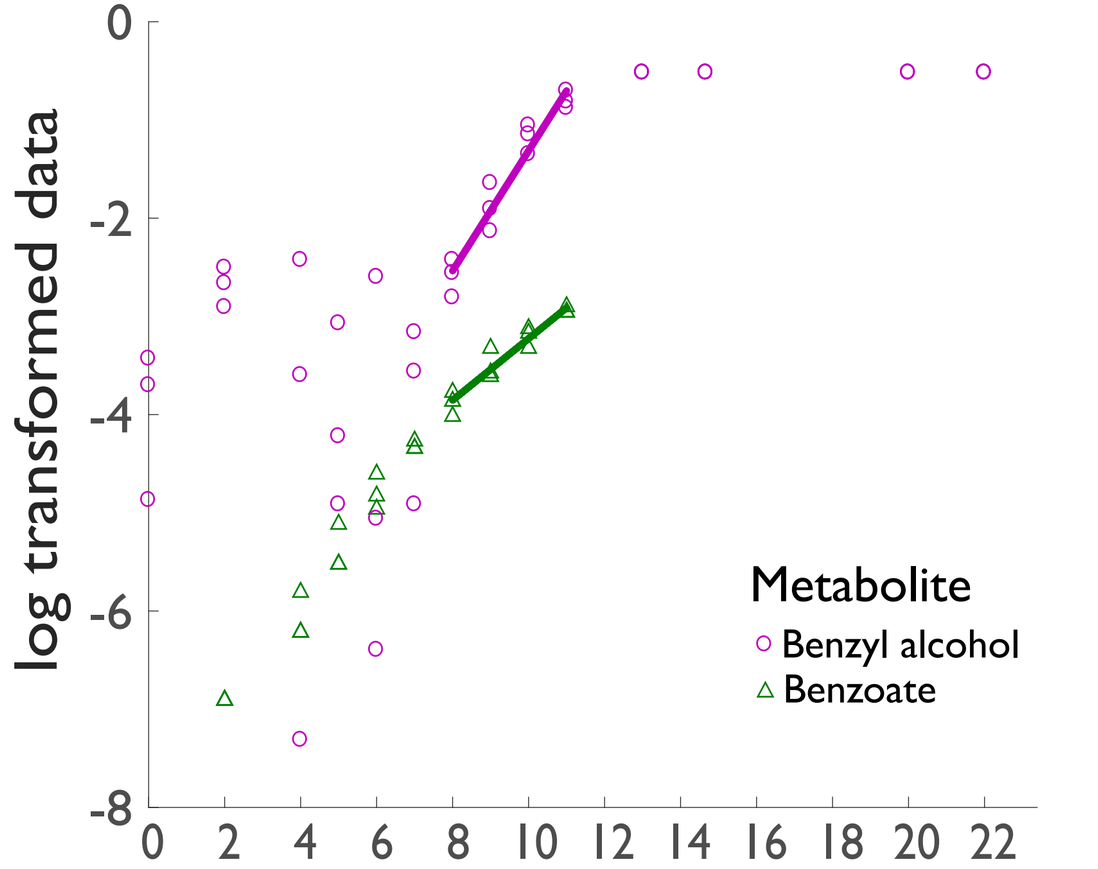

C

A. johnsonii growth in Benzyl Alcohol

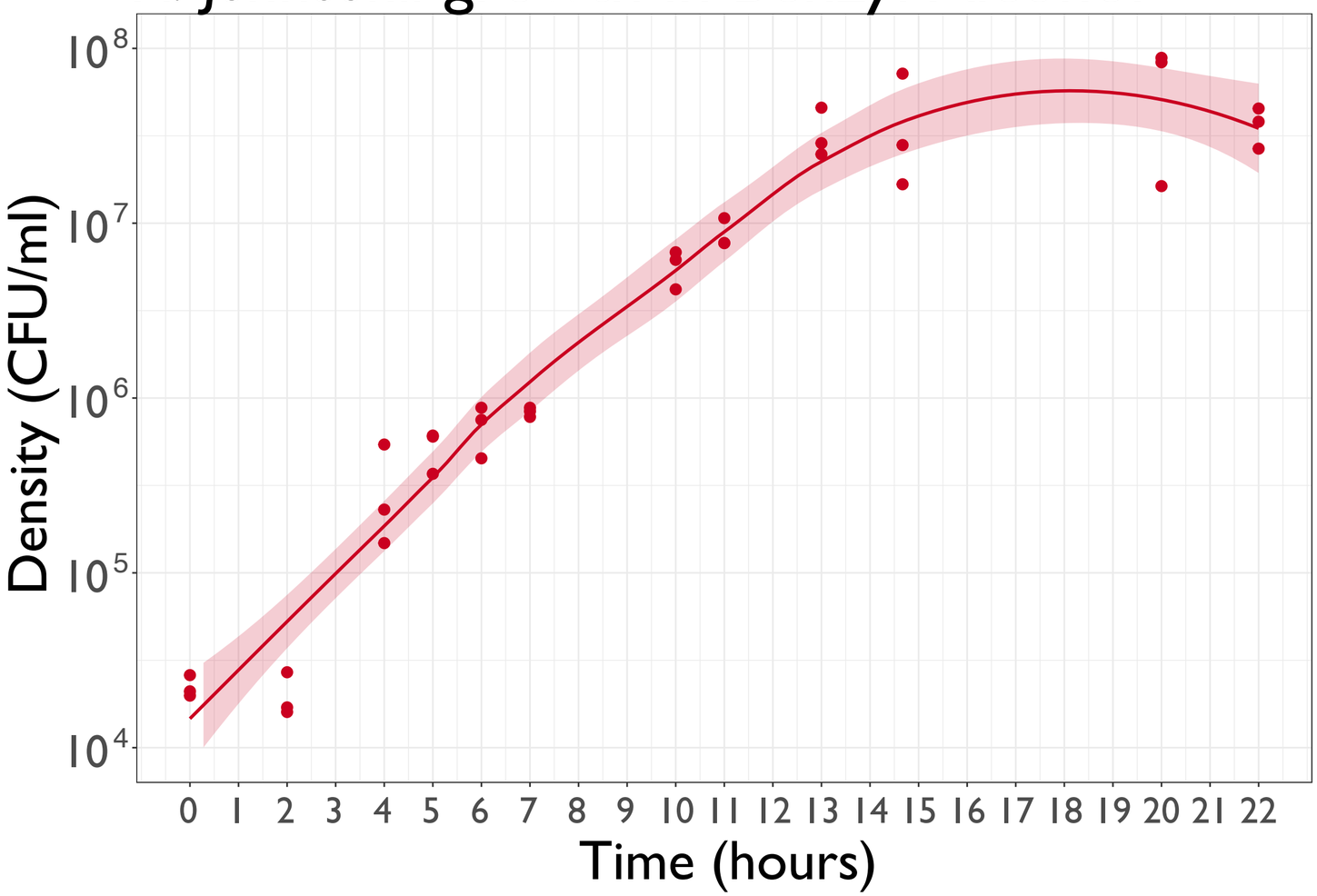

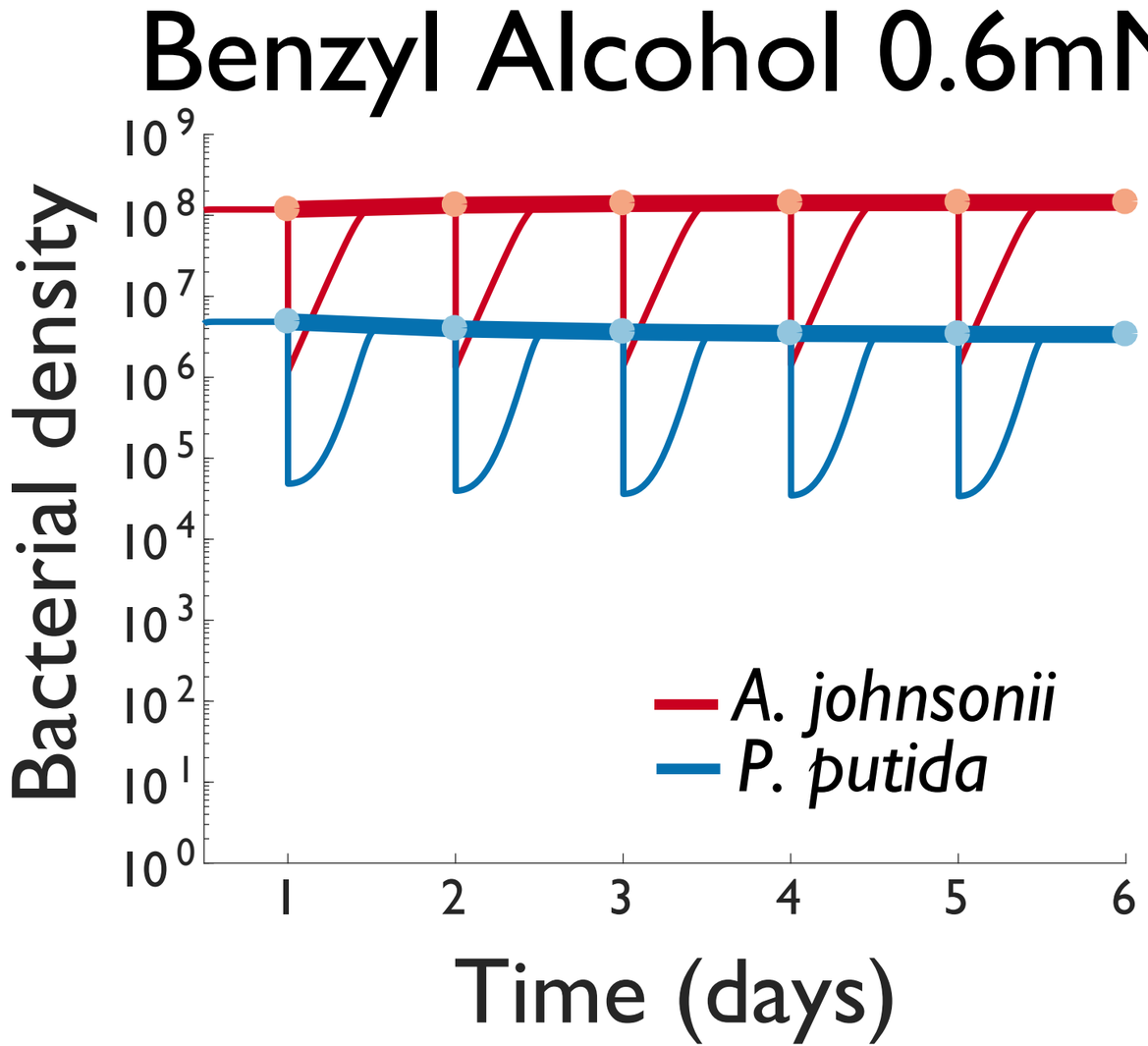
Benzyl Alcohol 0.6mM
Bacterial density
10^9
10^8
10^7
10^6
10^5
10^4
10^3
10^2
10^1
10^0
1
2
3
4
5
6
Time (days)
A. johnsonii
P. putida

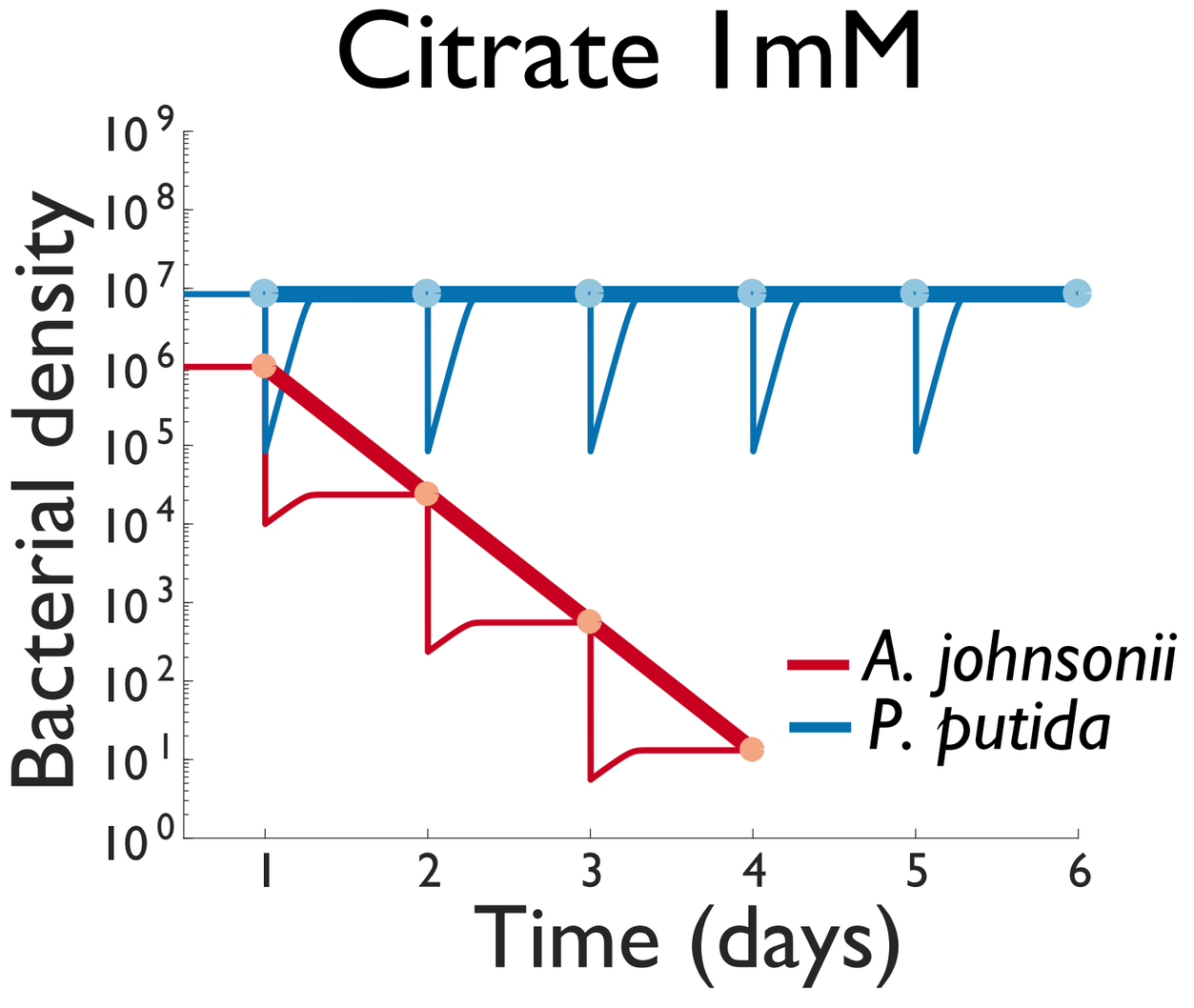
Citrate 1mM
Bacterial density
10^9
10^8
10^7
10^6
10^5
10^4
10^3
10^2
10^1
10^0
1
2
3
4
5
6
Time (days)
A. johnsonii
P. putida

6 days fluctuations